

# Filling factors and scale heights of the DIG in the Milky Way

E.M. BERKHUIJSEN, D. MITRA, and P. MÜLLER

Max-Planck-Institut für Radioastronomie, Auf dem Hügel 69, 53121 Bonn, Germany

Received 16 August 2005; accepted <date>; published online <date>

**Abstract.** The combination of dispersion measures of pulsars, distances from the model of Cordes & Lazio (2002) and emission measures from the WHAM survey enabled a statistical study of electron densities and filling factors of the diffuse ionized gas (DIG) in the Milky Way. The emission measures were corrected for absorption and contributions from beyond the pulsar distance. For a sample of 157 pulsars at  $|b| > 5^\circ$  and  $60^\circ < \ell < 360^\circ$ , located in mainly interarm regions within about 3 kpc from the Sun, we find that: **(1)** The average volume filling factor along the line of sight  $\bar{f}_v$  and the mean density in ionized clouds  $\bar{n}_c$  are inversely correlated:  $\bar{f}_v(\bar{n}_c) = (0.0184 \pm 0.0011)\bar{n}_c^{-1.07 \pm 0.03}$  for the ranges  $0.03 < \bar{n}_c < 2 \text{ cm}^{-3}$  and  $0.8 > \bar{f}_v > 0.01$ . This relationship is very tight. The inverse correlation of  $\bar{f}_v$  and  $\bar{n}_c$  causes the well-known constancy of the average electron density along the line of sight. As  $\bar{f}_v(z)$  increases with distance from the Galactic plane  $|z|$ , the average size of the ionized clouds increases with  $|z|$ . **(2)** For  $|z| < 0.9$  kpc the local density in clouds  $n_c(z)$  and local filling factor  $f(z)$  are inversely correlated because the local electron density  $n_e(z) = f(z)n_c(z)$  is constant. We suggest that  $f(z)$  reaches a maximum value of  $> 0.3$  near  $|z| = 0.9$  kpc, whereas  $n_c(z)$  continues to decrease to higher  $|z|$ , thus causing the observed flattening in the distribution of dispersion measures perpendicular to the Galactic plane above this height. **(3)** For  $|z| < 0.9$  kpc the local distributions  $n_c(z)$ ,  $f(z)$  and  $n_e^2(z)$  have the same scale height which is in the range  $250 < h \lesssim 500$  pc. **(4)** The average degree of ionization of the warm atomic gas  $\bar{T}_w(z)$  increases towards higher  $|z|$  similarly to  $\bar{f}_v(z)$ . Towards  $|z| = 1$  kpc,  $\bar{f}_v(z) = 0.24 \pm 0.05$  and  $\bar{T}_w(z) = 0.24 \pm 0.02$ . Near  $|z| = 1$  kpc most of the warm, atomic hydrogen is ionized.

**Key words:** Galaxy: disk – H II regions – ISM: clouds – ISM: structure

©0000 WILEY-VCH Verlag GmbH & Co. KGaA, Weinheim

## 1. Introduction

The interstellar medium (ISM) in galaxies largely consists of hydrogen that occurs in four different phases: the cold neutral medium (CNM: molecular gas and cold atomic gas), the warm neutral medium (WNM: warm atomic gas), the warm ionized medium (WIM) and the hot ionized medium (HIM). Near the Sun typical temperatures/densities of these phases are  $80 \text{ K}/40 \text{ cm}^{-3}$ ,  $8000 \text{ K}/0.4 \text{ cm}^{-3}$ ,  $8000 \text{ K}/0.2 \text{ cm}^{-3}$  and  $10^6 \text{ K}/0.003 \text{ cm}^{-3}$ , respectively (Kulkarni & Heiles 1988; Ferrière 1998), which shows that they have about equal thermal pressures. Physical processes like ionization and cooling depend on the structure of the ISM (i.e. diffuse, or cloudy, clumped), therefore the volume filling factors of the different phases as well as of the gas within these phases are important quantities.

Observations of external galaxies and the Milky Way showed that the warm and hot phases are extended and seem to occupy most of the interstellar space, whereas the CNM

fills only a small fraction (Kulkarni & Heiles 1988; Dickey 1993; Ferrière 1998). The WIM consists of dense classical H II regions and diffuse ionized gas (DIG) around and in between these regions. Also ionized surfaces of cool clouds may contribute to the DIG (Miller & Cox 1993). Walterbos & Braun (1994) described the wide-spread, diffuse H $\alpha$  emission visible in the spiral arms of M 31 as tori around the arms with negligible H $\alpha$  emission in between the arms.

Reynolds (1991b) obtained an exponential scale height of the DIG in the solar neighbourhood of about 900 pc from the increase of pulsar dispersion measures perpendicular to the Galactic plane with height above the plane. Scale heights near 1 kpc were also found by other authors using different pulsar samples (Bhattacharya & Verbunt 1991; Nordgren et al. 1992; Gómez et al. 2001; Cordes & Lazio 2003). The first estimates of the volume filling factor of this ionized layer were made by Reynolds (1977), who derived a lower limit to the filling factor of  $\simeq 0.1$  from the emission measures and dispersion measures in the direction of 24 pulsars at Galactic latitudes  $|b| > 5^\circ$  and a model of the ionized gas layer. In a

later paper (Reynolds 1991a) he used the dispersion measures and emission measures towards 4 pulsars in globular clusters about 3 kpc away from the midplane of the disk. He found a mean filling factor of  $\gtrsim 0.2$  which represents an average value through the full layer. The ionized gas appeared to be concentrated in extended clouds of mean density  $0.08 \text{ cm}^{-3}$  occupying about 200 pc along a line of sight towards the Galactic pole.

Maps of neutral and ionized gas of the Milky Way and other edge-on galaxies show that bright, dense clouds are concentrated to a thin disk that is surrounded by extended, diffuse emission from less dense gas reaching large distances from the galaxy plane. This indicates that there is an anticorrelation between gas density and area filling factor with the latter increasing away from the plane. In the Milky Way the volume density of the atomic gas decreases with increasing distance from the Galactic plane (Dickey & Lockman 1990), thus the ionized gas density may also decrease and its volume filling factor may increase. Kulkarni & Heiles (1988) estimated the variation of the local volume filling factor,  $f$ , and the local mean density within ionized clouds,  $n_c$ , with distance from the plane,  $z$ , assuming exponential functions for the local electron densities  $n_e$  and  $n_e^2$ . They obtained  $f(z) \simeq 0.11 \exp(|z|/640 \text{ pc})$  and  $n_c(z) = 0.27 \exp(-|z|/360 \text{ pc}) \text{ cm}^{-3}$ , scaled to a Galactic centre distance of 8.5 kpc. The local volume filling factor then increases from 0.11 at  $z = 0 \text{ pc}$  to 0.52 at  $|z| = 1 \text{ kpc}$ . At  $|z| = 400 \text{ pc}$ , about half the scale height of the DIG,  $f \simeq 0.21$  and  $n_c \simeq 0.08 \text{ cm}^{-3}$ , in agreement with Reynold's (1991a) results.

The relationship between the average volume filling factor  $\bar{f}_v$  and mean electron density within clouds  $\bar{n}_c$ , both averaged along the line of sight, carries important information on the structure of the DIG. For example, Elmegreen (1998, 1999) showed that turbulence causing hierarchical, fractal structure leads to an inverse relationship between  $\bar{f}_v$  and  $\bar{n}_c$ . Pynzar (1993) was the first to investigate this relationship, not only for the DIG but also for the classical H II regions. He used dispersion measures and emission measures towards pulsars and observations of recombination lines from dense H II regions. These data yielded  $\bar{f}_v(\bar{n}_c) \propto \bar{n}_c^{-0.7}$ . Estimates for a mixture of spiral arm and interarm regions by Heiles et al. (1996) and Berkhuijsen (1998) are in agreement with Pynzar's result (see compilation by Berkhuijsen 1998). An inverse relationship between  $\bar{f}_v$  and  $\bar{n}_c$  is indicated by the near constancy of the average electron density along the line of sight  $\langle n_e \rangle$  derived from dispersion measures of pulsars with known distances. The constancy of  $\langle n_e \rangle$  was first pointed out by Weisberg et al. (1980); although it is widely used to derive pulsar distances, its physical significance did not attract attention.

Recently, a new masterlist of pulsar data has become available (Hobbs & Manchester 2003). We used the dispersion measures of pulsars at Galactic latitudes above  $|5^\circ|$  in this list together with emission measures from the Wisconsin H $\alpha$  Mapper (WHAM, Haffner et al. 2003), corrected for absorption and for contributions from beyond the pulsars, for an improved determination of the relationship between  $\bar{f}_v$  and

$\bar{n}_c$  in the DIG. The distances of the pulsars we took from the new model of the electron distribution in the Galaxy presented by Cordes & Lazio (2002). In this sample of several hundred pulsars we also searched for variations of  $\bar{f}_v$  and  $\bar{n}_c$  with  $z$  in the DIG, determined their exponential scale heights and derived the scale heights of the local functions  $f(z)$  and  $n_c(z)$ .

The paper is organized as follows: In Sect. 2 we describe the derivation of  $\bar{f}_v$  and  $\bar{n}_c$  and the data used. In Sect. 3 we explain the statistical procedure and describe the results, which are discussed in Sect. 4. Section 5 gives a summary of our conclusions. Appendix A contains a glossary of the variables used. A table listing relevant parameters of the pulsars in the final sample is available on request<sup>1</sup>.

## 2. Basic relations and data used

### 2.1. Basic relations

The expressions for dispersion measure, DM, and emission measure, EM, towards a pulsar at a distance  $D$  (in pc) can be written in several ways:

$$\frac{\text{DM}}{\text{cm}^{-3} \text{ pc}} = \int_0^D n_e(l) dl = \langle n_e \rangle D = \bar{n}_c \bar{f}_D D = \bar{n}_c L_e, \quad (1)$$

$$\frac{\text{EM}}{\text{cm}^{-6} \text{ pc}} = \int_0^D n_e^2(l) dl = \langle n_e^2 \rangle D = \bar{n}_c^2 \bar{f}_D D = \bar{n}_c^2 L_e, \quad (2)$$

where  $n_e(l)$  (in  $\text{cm}^{-3}$ ) is the electron density at a point  $l$  along the line of sight,  $L_e$  (in pc) the total path length through the regions containing free electrons (clouds) and  $\bar{n}_c$  (in  $\text{cm}^{-3}$ ) the average density in these regions which is the mean density of a cloud if constant for all clouds along the line of sight (see Fig. 1). Furthermore,  $\langle n_e \rangle$  and  $\langle n_e^2 \rangle$  are averages along  $D$  and  $\bar{f}_D = L_e/D$  is the fraction of the line of sight occupied by electrons. Note that all quantities with overbars are averages along a line of sight.<sup>2</sup>

Combining Eqs. (1) and (2) we find

$$\bar{f}_D = \frac{L_e}{D} = \frac{\langle n_e \rangle}{\bar{n}_c} = \frac{\langle n_e^2 \rangle}{\bar{n}_c^2} \quad (3)$$

Other useful expressions are:

$$\bar{n}_c = \frac{\text{DM}}{L_e} = \frac{\text{EM}}{\text{DM}}, \quad L_e = \frac{\text{DM}^2}{\text{EM}} \quad \text{and} \quad \bar{f}_D = \frac{\text{DM}^2}{\text{EM} \cdot D}. \quad (4)$$

It is not a priori clear whether the line-of-sight filling factor  $\bar{f}_D$  is the same as the volume filling factor  $\bar{f}_v$  that we want to measure. The volume filling factor is the fraction of the observed volume occupied by the clouds. Generally,  $\bar{f}_v = c \bar{f}_D$ , where  $c$  is a factor depending on distance, size and shape of the clouds. Looking towards a pulsar, the observed volume is the volume of the radio beam out to the distance of the pulsar. The volume of this cone is  $V_{\text{beam}} = \frac{\pi}{3} D (D \tan \frac{\theta}{2})^2$ , where  $\theta$  is the half-power beamwidth in degrees. As  $\theta$  is small,

<sup>1</sup> eberkhuijsen@mpifr-bonn.mpg.de

<sup>2</sup> We keep the conventional forms  $\langle n_e \rangle$  and  $\langle n_e^2 \rangle$ , but use overbars for other averaged variables to clearly distinguish similar quantities and to simplify the notation.

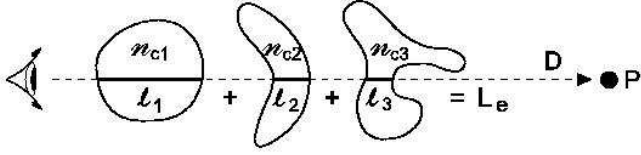


**Fig. 1.** Three ionized clouds along the line of sight towards a pulsar  $P$  at distance  $D$ . The path lengths through the clouds –  $l_1$ ,  $l_2$  and  $l_3$  – are indicated by thick lines. The total path length filled with electrons is  $L_e = l_1 + l_2 + l_3$  and the filling fraction  $\bar{f}_D = L_e/D$ . The local electron densities within the clouds –  $n_{c1}$ ,  $n_{c2}$  and  $n_{c3}$  – give a mean density in clouds  $\bar{n}_c = (n_{c1}l_1 + n_{c2}l_2 + n_{c3}l_3)/L_e$ . The average electron density along the line of sight is  $\langle n_e \rangle = (n_{c1}l_1 + n_{c2}l_2 + n_{c3}l_3)/D$ . Thus  $\langle n_e \rangle = \bar{f}_D \bar{n}_c$ . If  $\bar{f}_D$  represents the average volume filling factor  $\bar{f}_v$  (see Sect. 2.1),  $\langle n_e \rangle = \bar{f}_v \bar{n}_c$ .

$\tan \frac{\theta}{2} = \frac{d}{2D}$  and  $V_{\text{beam}} = \frac{\pi}{12} D d^2$ , where  $d$  is the linear size of the beam at distance  $D$ . A thin cloud at distance  $D$  and of thickness  $l \ll D$  along the line of sight, more extended than the beamwidth, occupies  $V_c \simeq \frac{\pi}{12} l d^2$ , so in this case indeed  $\bar{f}_v \simeq \bar{f}_D = l/d$  and  $c \simeq 1$ . Similarly,  $c \simeq 2$  for a spherical cloud of diameter  $d$  equal to the beamwidth, located near the pulsar, and  $c \lesssim 1$  for spherical clouds of diameter  $l \lesssim d^{1/3}$ . As the DIG mainly consists of filaments and sheets (Reynolds 1991b), we could assume  $c \simeq 1$  and  $\bar{f}_D = \bar{f}_v$ . However, an extended sheet located close to the pulsar will occupy a larger fraction of the beam volume than a similar cloud near the observer. On average, clouds will be situated about half-way to the pulsar, near  $D/2$ . Then for a cloud thickness  $l = \bar{f}_D D$  the cloud volume is  $V_c = \frac{\pi}{96} D d^2 [(1 + \bar{f}_D)^3 - (1 - \bar{f}_D)^3]$  and  $\bar{f}_v = V_c/V_{\text{beam}} = \frac{1}{8} [(1 + \bar{f}_D)^3 - (1 - \bar{f}_D)^3]$ . This gives  $c = \bar{f}_v/\bar{f}_D = 0.75$  for  $\bar{f}_D \lesssim 0.15$  with a slow increase to  $c = 1$  for larger values of  $\bar{f}_D$ .

In most directions there will be several clouds or sheets along the line of sight with a total thickness  $L_e$  that is centred near  $D/2$ . Therefore we conclude that generally  $\bar{f}_D \simeq \bar{f}_v$  and we will use  $\bar{f}_v$  in the remaining of the paper.

## 2.2. The data

In order to obtain realistic values for  $\bar{n}_c$  and  $\bar{f}_v$  from Eqs. (1) to (4) DM and EM should arise in the same ionized regions in front of the pulsar. For nearby pulsars at low Galactic latitudes a considerable amount of the observed emission measure EM may originate beyond the distance of the pulsar, whereas for pulsars at large distances absorption may reduce EM. Near the Galactic plane classical H II regions on the line of sight towards the pulsar may also influence the results (Mitra et al. 2003). To minimize these problems we used pulsars at Galactic latitudes  $|b| > 5^\circ$ .

The dispersion measures of the pulsars were taken from the catalogue of Hobbs & Manchester (2003). Among them are 19 pulsars with accurate parallactic distances (Brisken et al. 2002). We checked their positions for bright H II regions, which were found towards 6 of them. We used the 13 distance

calibrators left for comparison with a much larger sample. Of these 13 pulsars 8 are at  $|b| > 5^\circ$ .

The emission measures were taken from the WHAM Northern Sky Survey (Haffner et al. 2003). This data set represents the total H $\alpha$  intensity, integrated between LSR velocities  $-80$  and  $+80$  km/s, within a one-degree diameter beam centred at a specified position. The intensities and errors are given in Rayleighs ( $10^6/4\pi$  photons  $\text{cm}^{-2} \text{s}^{-1} \text{sr}^{-1}$ ); the sensitivity of the survey is 0.1R. At the H $\alpha$  wavelength  $1R = 2.41 \cdot 10^{-7}$  erg  $\text{cm}^{-2} \text{s}^{-1} \text{sr}^{-1}$  which is equivalent to  $EM = 2.25 \text{ cm}^{-6} \text{ pc}$  for  $T_e = 8000$  K, the mean electron temperature in the DIG. A possible increase of  $T_e$  with increasing  $|z|$  (Haffner et al. 1999) will hardly influence emission measures observed through the disk at  $|b| > 5^\circ$ . For the interpolation of these data to a pulsar position we used a modified quadratic Shepard method for interpolation of scattered data in a plane and quadratic error propagation. With the constraint  $|b| > 5^\circ$  the overlap between the pulsar catalogue and WHAM survey yields a sample of 320 pulsars.

In Fig. 2 we plot EM and DM as a function of Galactic latitude. The sharp rise in both EM and DM at  $|b| < 5^\circ$  is due to the classical H II regions and increasing lines of sight. In most cases  $EM < DM$ , which indicates that generally  $\bar{n}_c < 1 \text{ cm}^{-3}$ . For all further analyses we excluded 30 more pulsars from our  $|b| > 5^\circ$  sample based on the fact that they deviate significantly from the outer envelope of the EM distribution. We also excluded pulsars located in the Magellanic clouds and in globular clusters. Our sample at  $|b| > 5^\circ$  then consisted of 285 pulsars including 8 of the 13 distance calibrators. The relevant parameters of the 13 calibrators are listed in Table 1.

We determined the distances towards the pulsars in our sample from the new model of the electron distribution in the Galaxy of Cordes & Lazio (2002) which is the most realistic model presently available. Although its basic structure (i.e. thick disk, thin disk, spiral arms) is nearly identical to that of the older models of Taylor & Cordes (1993) and Gómez et al. (2001), it contains more detail resulting from the larger data sets of various kinds on which it is based (i.e. not only on dispersion measures, but also on scattering measures as well as optical and X-ray observations). Therefore this model performs considerably better than the earlier models (see Table 1 in Cordes & Lazio (2003). It is well defined for the pulsars in our final sample, which are at  $|b| > 5^\circ$  and within about 3 kpc from the Sun in mainly interarm regions (see Fig. 4). The statistical error in the model distances is about 20% (Cordes & Lazio 2002, their Fig. 12), which is much smaller than the intrinsic spread in the observed dispersion measures (s.d. of factor 2) and emission measures (s.d. of factor 4, see Fig. 7). This means that the errors in the model distances are *negligible* in our statistical study of the relationship between the electron density in clouds and filling factors in the DIG, and of their variation with height above the Galactic plane.

## 2.3. Corrections to emission measures

The emission measures observed in the directions of the pulsars are not the ideal values for obtaining filling factors and

**Table 1.** Parameters of 13 pulsars with parallactic distances

PSR Jname	$\ell$ [ $^\circ$ ]	$b$ [ $^\circ$ ]	DM <sup>1)</sup> [cm <sup>-3</sup> pc]	$D^{2)}$ [kpc]	$ z_p $ [kpc]	EM [cm <sup>-6</sup> pc]	EM <sub>p</sub> <sup>3)</sup> [cm <sup>-6</sup> pc]	$\bar{n}_c$ [cm <sup>-3</sup> ]	$\bar{f}_v$
J0332+5434	145.0	-1.2	26.78	1.03 <sup>+0.13</sup> <sub>-0.12</sub>	0.022±0.003	10.0±2.9	46±18	1.7 ±0.7	0.015±0.006
J0814+7429	140.0	31.6	5.75	0.433±0.008	0.227±0.004	1.79±0.03	1.2±0.1	0.20±0.02	0.065±0.005
J0953+0755	228.9	43.7	2.97	0.262±0.005	0.181±0.003	3.6±0.9	1.9±0.5	0.65±0.17	0.017±0.005
J1136+1551	241.9	69.2	4.85	0.35 ±0.02	0.327±0.019	1.5±0.4	1.1±0.3	0.23±0.06	0.059±0.017
J1932+1059	47.4	-3.9	3.18	0.331±0.010	0.023±0.001	10.5±1.1	2.9±0.5	0.92±0.16	0.010±0.002
J2018+2839	68.1	-4.0	14.18	0.95 ±0.09	0.066±0.006	13.2±0.2	9.5±1.4	0.67±0.10	0.022±0.004
J2022+2854	68.9	-4.7	24.62	2.3 <sup>+1.0</sup> <sub>-0.6</sub>	0.19 <sup>+0.08</sup> <sub>-0.05</sub>	18.2±1.2	25.4±3.1	1.03±0.13	0.010 <sup>+0.005</sup> <sub>-0.003</sub>
J2022+5154	87.9	8.4	22.58	1.9 <sup>+0.3</sup> <sub>-0.2</sub>	0.28 <sup>+0.04</sup> <sub>-0.03</sub>	10.5±2.1	11.9±2.5	0.53±0.11	0.023 <sup>+0.006</sup> <sub>-0.005</sub>
J0922+0638	225.4	36.4	27.31	1.15 <sup>+0.21</sup> <sub>-0.16</sub>	0.68 <sup>+0.12</sup> <sub>-0.09</sub>	6.4±1.1	6.7±1.2	0.24±0.04	0.097 <sup>+0.025</sup> <sub>-0.022</sub>
J1537+1155	19.9	48.3	11.62	1.08 <sup>+0.16</sup> <sub>-0.14</sub>	0.81 <sup>+0.12</sup> <sub>-0.10</sub>	2.7±0.2	2.9±0.2	0.25±0.02	0.044 <sup>+0.007</sup> <sub>-0.006</sub>
J1857+0943	42.3	3.1	13.31	0.79 <sup>+0.29</sup> <sub>-0.17</sub>	0.043 <sup>+0.015</sup> <sub>-0.009</sub>	18.6±2.9	13.0 <sup>+5.0</sup> <sub>-3.7</sub>	0.98 <sup>+0.37</sup> <sub>-0.28</sub>	0.017 <sup>+0.009</sup> <sub>-0.006</sub>
J1713+0747	28.8	25.2	15.99	0.90 <sup>+0.04</sup> <sub>-0.02</sub>	0.383 <sup>+0.017</sup> <sub>-0.009</sub>	4.3±0.2	3.9±0.3	0.25±0.02	0.072±0.006
J1744-1134	14.8	9.2	3.14	0.35 <sup>+0.03</sup> <sub>-0.02</sub>	0.056 <sup>+0.005</sup> <sub>-0.003</sub>	12.0±0.3	3.7 <sup>+0.5</sup> <sub>-0.4</sub>	1.19 <sup>+0.16</sup> <sub>-0.14</sub>	0.008±0.001

<sup>1)</sup> Taylor et al. (1993), errors are  $\lesssim 1\%$ ; <sup>2)</sup> Brisken et al. (2002)

<sup>3)</sup> Emission measure in front of the pulsar, corrected for absorption (see Sect. 2.3). Errors are one standard deviation

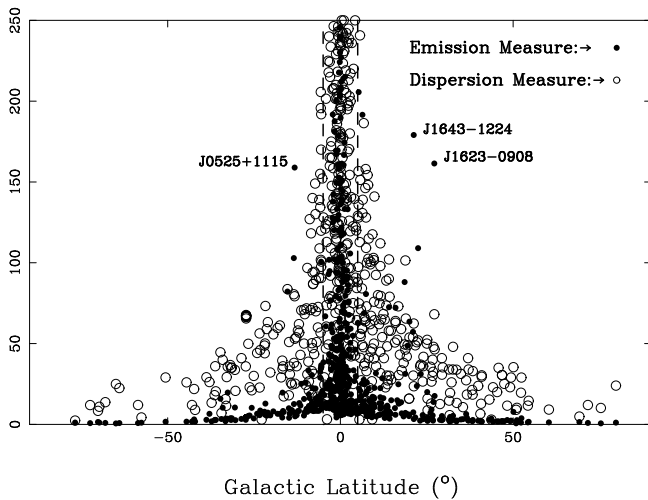


**Fig. 2.** Latitude distribution of observed dispersion measures and emission measures towards 744 pulsars in the field of the WHAM survey (Haffner et al. 2003), from which the emission measures were taken. The dashed lines are at  $b = \pm 5^\circ$ . Some pulsars with exceptionally high emission measures are indicated.

electron densities from Eqs. (1) to (4). On the one hand they are too small because of absorption of the H $\alpha$  emission by dust along the line of sight, while on the other hand they are too large because of contributions from distances beyond the pulsars. We have developed approximate corrections for these two competing effects.

First we correct the observed emission measures for absorption. Following Haffner et al. (1998), the corrected emission measure is

$$\text{EM}_c = \text{EM} \cdot A \quad \text{with } A = e^{2.2E(B-V)},$$

where  $E(B - V)$  is the colour excess along the line of sight. We can estimate  $E(B - V)$  from the results of Diplas &

Savage (1994) who obtained  $E(B - V) \sin |b|$  as a function of distance  $|z|$  above the Galactic plane for a large number of stars. As they selected stars seen through the diffuse ISM, avoiding dust clouds, their result is especially suited for correcting the emission measures from the DIG. They derived an exponential scale height of the dust layer of  $152 \pm 7$  pc and  $[E(B - V)/\text{kpc}] = 0.257 \pm .010 \text{ mag kpc}^{-1}$  in the Galactic plane. Integration of this function to infinite  $|z|$  yields  $E(B - V) \sin |b| = (0.0391 \pm 0.0024)$  and  $A = \exp((0.086 \pm 0.005)/\sin |b|)$ . As our sample only contains pulsars at  $|b| > 5^\circ$ , the largest value of  $A = 2.68 \pm 0.16$  (see Fig. 5) and we expect that the observed and corrected emission measures contain contributions from all distances along the line of sight through the electron layer. The data of Diplas & Savage (1994) show considerable spread around their fitted line which they attribute to inhomogeneities in the dust distribution. These will cause variations in the absorption of the H $\alpha$  emission and extra spread in the observed emission measures.<sup>3</sup>

Since we expect that  $\text{EM}_c$  contains contributions from the full line of sight through the electron layer,  $\text{EM}_c \sin |b|$  for a pulsar represents the absorption-free emission measure of the full layer perpendicular to the Galactic plane at the distance of the pulsar. It will vary among pulsars due to spread in the data and true variations in electron density with position. But if the absorption correction is applicable, the values of  $\text{EM}_c \sin |b|$  for the pulsar sample should be independent of  $|z|$ . We checked this for our total sample and found no dependence on  $|z|$  for longitudes  $\ell > 60^\circ$ , but a significant decrease of  $\text{EM}_c \sin |b|$  with  $|z|$  for  $0^\circ < \ell < 60^\circ$  (see Fig. 3). This could be due to unusual absorption along these lines of

<sup>3</sup> The function of  $A$  derived from the work of Diplas & Savage (1994) at  $|b| \gtrsim 10^\circ$  is consistent with Eq. 1 given by Dickinson et al. (2003) which is based on the dust map of Schlegel et al. (1998). At lower latitudes our values are smaller than those of Dickinson et al., because we only consider diffuse dust.

sight. The area contains an extended dust cloud with high  $E(B - V)/\text{kpc}$  at 300 pc distance from the Sun (Sherwood 1974; Lucke 1978) and a chain of dense molecular clouds known as the Aquila Rift (Dame et al. 2001) extending to  $b > +10^\circ$ . As more than 70% of the pulsars at  $0^\circ < \ell < 60^\circ$  are at  $|b| < 15^\circ$ , many lines of sight will cut through dust clouds. In a plot of EM against longitude the effect of the dust clouds is clearly visible as a deep minimum centred on  $\ell = 40^\circ$  which does not occur in the dispersion measures. Such disagreement is not seen at  $\ell > 60^\circ$ . Because the absorption correction taken from Diplás & Savage (1994) only applies to the diffuse dust, we had to omit 128 pulsars in the range  $0^\circ < \ell < 60^\circ$ ,  $b > -15^\circ$  from our sample, leaving 157 pulsars at  $|b| > 5^\circ$  for further analysis. Of these, 14 pulsars are at  $0^\circ < \ell < 60^\circ$ ,  $b < -15^\circ$ . Only 5 distance calibrators of Table 1 are left in the sample. The distribution of these 157 pulsars projected on the Galactic plane is shown in Fig. 4. Most of the pulsars in our final sample are located in interarm regions and within about 3 kpc from the Sun.

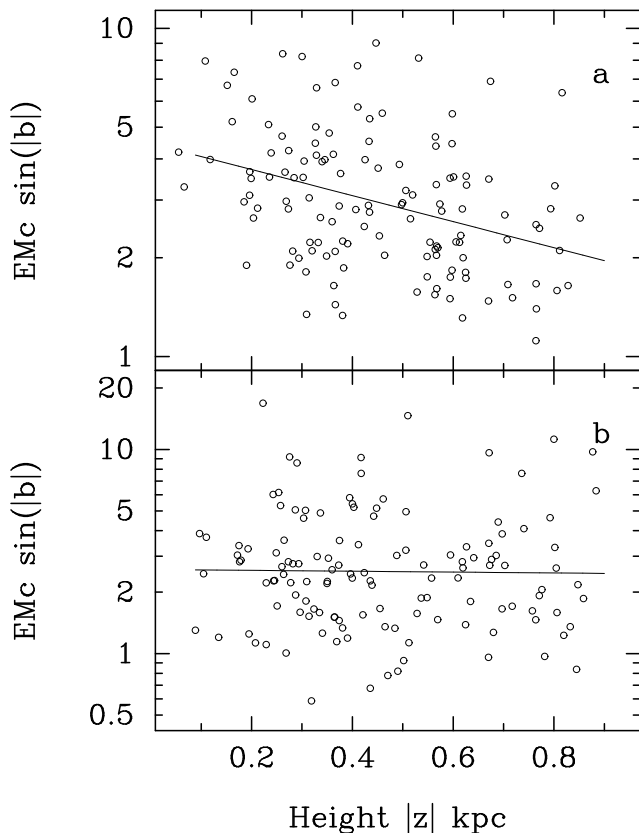


**Fig. 3.** Dependence of the emission measures (in  $\text{cm}^{-6} \text{pc}$ ) perpendicular to the Galactic plane, corrected for absorption, on distance to the plane. The full lines are least-squares regression lines of  $\log(\text{EM}_c \sin |b|)$  on  $|z|$ . If the absorption corrections are adequate  $\text{EM}_c \sin |b|$  should be independent of  $|z|$  as is the case for pulsars at  $60^\circ < \ell < 360^\circ$  (**b**), but not for pulsars at  $0^\circ < \ell < 60^\circ$  (**a**) where the slope of the line is significant ( $-0.40 \pm 0.09$ ).

Next we determine which part of the corrected emission measure originates in front of the pulsar. The absorption-

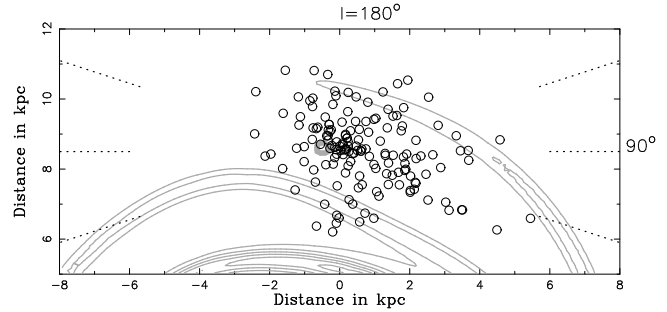


**Fig. 4.** Distribution of the final sample of 157 pulsars projected on the Galactic plane. Full lines are contours of electron density from the model of Cordes & Lazio (2002). Dotted lines indicate Galactic longitude. The Sun is located at 8.5 kpc from the Galactic centre.

corrected emission measure increases with distance from the Galactic plane as

$$\text{EM}_c(z) \sin |b| = \int_0^{|z|} n_e^2(z) dz = \int_0^{|z|} n_e^2(0) e^{-|z|/h} dz, \quad (5)$$

where  $n_e^2(0)$  is the value of  $n_e^2(z)$  at  $|z| = 0$  pc and  $h$  is the exponential scale height. The fraction of the total emission measure towards the pole coming from the layer below the  $|z|$ -distance of the pulsar,  $|z_p|$ , is the ratio of Eq. (5) integrated to  $|z_p|$  and that integrated through the full layer. Hence, in front of the pulsar originates

$$\text{EM}_p \sin |b| = \text{EM}_c \sin |b| \cdot (1 - e^{-|z_p|/h}). \quad (6)$$

At this point we do not know the scale height  $h$ , but we do know that the mean value of  $\text{EM}_c \sin |b|$  for all pulsars should equal  $\overline{n_e^2(0)h}$  for the sample considered. In Sect. 4.1 we combine  $\overline{\text{EM}_c \sin |b|}$  with information on  $\text{DM} \sin |b|(z)$  to evaluate  $h$ , which appears to be in the range  $250 < h < 500$  pc. The minimum value of  $280 \pm 30$  pc is best constrained. Therefore we used  $h = 280$  pc in Eq. (6). A larger value of  $h$  leads to a smaller value of the correction factor  $B = 1 - e^{-|z_p|/h}$ . We show in Sect. 3.5 that our results are not very sensitive to the choice of  $h$  in the range  $250 < h < 500$  pc.

In Fig. 5 we illustrate the effect of the two corrections to EM for pulsars at different latitudes and distances. Especially for pulsars at low  $|z|$  (i.e. small  $D$ , low  $b$ ) the correction for the contribution to EM from beyond the pulsar dominates the absorption correction leading to  $\text{EM}_p < \text{EM}$ .

The final sample of 157 pulsars projected on the WHAM survey is shown in Fig. 6. A table collecting the properties of these pulsars is available on request<sup>4</sup>.

### 3. Results

In this section we compare the observed as well as the corrected EM with the DM towards the 157 pulsars in our sample (Sect. 3.1), derive the exponential scale heights of  $\langle n_e \rangle$ ,  $\langle n_e^2 \rangle$ ,  $\overline{n}_c$  and  $\overline{f}_v$  (Sect. 3.2), and present the relationship between  $\overline{f}_v$  and  $\overline{n}_c$  (Sect. 3.3).

<sup>4</sup> eberkhuijsen@mpifr-bonn.mpg.de

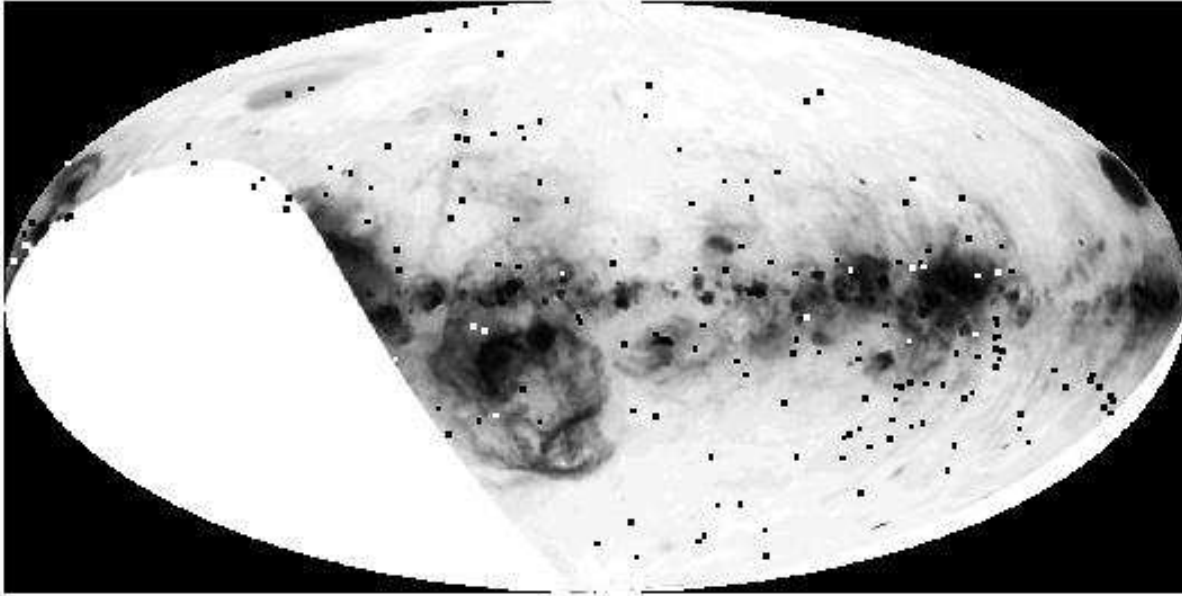


**Fig. 6.** Positions of the 157 pulsars in the final sample (filled squares) projected onto the distribution of the H $\alpha$  emission (WHAM survey, Haffner et al. 2003). The map is centred at  $\ell = 180^\circ$ ,  $b = 0^\circ$  and  $\ell = 0^\circ$  is at the right-hand border.

As EM and DM do not directly depend on each other, a symmetrical–statistical treatment is needed to find their relationship. Therefore we calculated the ordinary least-squares bisector in the log–log plane (Isobe et al. 1990) using the modified program code distributed by Feigelson. In all other cases we derived the ordinary least-squares regression line of  $Y$  on  $X$  in the relevant units. The quality of a correlation can be judged from the correlation coefficient  $r$  and the value of  $t$  resulting from the Student  $t$ -test, which gives the probability that the correlation is accidental. The correlation is highly significant at the  $3\sigma$  level if  $t > 3.1$  for a number of independent points  $N > 100$ . The values of  $r$ , the standard deviation in  $r$ ,  $\sigma_r$ , and  $t$  are calculated from the equations

$$r = \frac{\sum_1^N (X_i - \bar{X})(Y_i - \bar{Y})}{N\sigma_X\sigma_Y}, \quad \sigma_r = \sqrt{\frac{1-r^2}{N-2}},$$

$$t = r\sqrt{\frac{N-2}{1-r^2}},$$

where  $\bar{X}$  and  $\bar{Y}$  are the mean values of  $X$  and  $Y$ , respectively, and  $\sigma_X$  and  $\sigma_Y$  the standard deviations in  $X$  and  $Y$ . The measurement errors in EM and DM are small compared to the uncertainty of  $\lesssim 20\%$  in  $D$  (Cordes & Lazio 2002). Since all these errors are much smaller than the intrinsic scatter of the points ( $\gtrsim$  factor 2), all points were given equal weight in the fitting procedures. The results are listed in Table 2.

### 3.1. Dispersion measures and emission measures

If EM and DM occur in the same ionized regions along the line of sight, we expect  $\text{EM} = \bar{n}_c \text{DM}$ , or  $\text{EM} \propto \text{DM}^b$  with  $b > 1$ . To test this we plot in Fig. 7a the uncorrected emission measures EM as a function of DM and in Fig. 7b the corrected emission measures  $\text{EM}_p$  against DM for all 157 pulsars at  $|b| > 5^\circ$ . The corrections made to EM have clearly reduced the spread in the data. The bisector fit in Fig. 7b yields

$\text{EM}_p \propto \text{DM}^{1.47 \pm 0.09}$  and with  $r = 0.76$  and  $t = 15$  the correlation is highly significant. Because of the even distribution in latitude of the pulsars and the large fraction of pulsars (72%) at  $D > 1$  kpc, the slope of the bisector has not changed after the corrections to EM (see Table 2). Note that the components parallel to the Galactic plane,  $\text{EM}_p \cos |b|$  and  $\text{DM} \cos |b|$ , are even better correlated with nearly the same exponent.

Pynzar (1993) obtained  $\text{EM} \propto \text{DM}^2$  from the lower envelope to the data in his sample. This much steeper slope could be due to an increasing overestimate of the emission measures towards pulsars at large distances. Overestimates of EM could arise from the properties of the spiral arm model used by him or from contributions to EM from H II regions along the line of sight, especially as two thirds of the pulsars he used are at latitudes below  $|5^\circ|$ .

The variations of  $\text{DM} \sin |b|$  and  $\text{EM}_p \sin |b|$  with height above the Galactic plane,  $|z|$ , depend on the vertical distribution of the ionized gas. Figure 8a shows that  $\text{DM} \sin |b|$  continuously increases up to  $|z| \simeq 0.9$  kpc and then levels off. This behaviour reflects that of the more than 100 pulsars with independent distance estimates on which the model of Cordes & Lazio (2002) is partly based. A power-law fit to the data in Fig. 8a for  $|z| < 0.9$  kpc yields  $\text{DM} \sin |b| = (22.1 \pm 1.3) |z|_{\text{kpc}}^{1.04 \pm 0.05} \text{ cm}^{-3} \text{ pc}$  and is highly significant (see Table 2).

Figure 8b shows that  $\text{EM}_p \sin |b|$  also increases with  $|z|$  although not as strongly as  $\text{DM} \sin |b|$ . The power-law fit for  $|z| < 0.9$  kpc gives  $\text{EM}_p \sin |b| = (2.78 \pm 0.28) |z|_{\text{kpc}}^{0.46 \pm 0.11} \text{ cm}^{-6} \text{ pc}$  with high significance. It is not clear whether  $\text{EM}_p \sin |b|$  increases beyond  $|z| > 1$  kpc, because of the large spread. The value of  $\text{EM}_c \sin |b|$  for the 130 pulsars at  $|z| < 0.9$  kpc is  $3.18 \pm 0.19 \text{ cm}^{-6} \text{ pc}$ . Without absorption correction the mean value of  $\text{EM} \sin |b|$  is  $2.18 \pm$

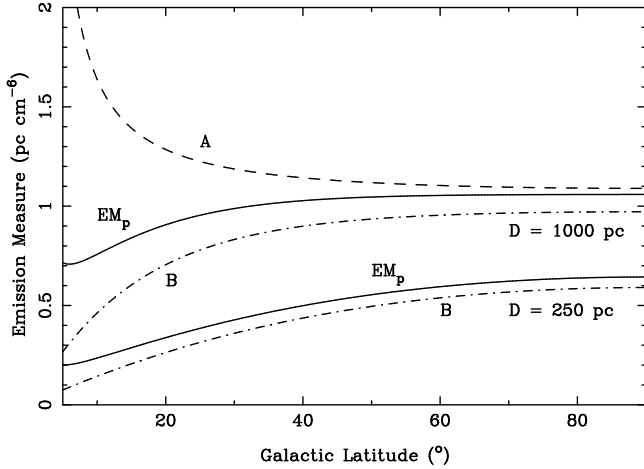


**Fig. 5.** Examples of the corrections to the observed emission measure as a function of Galactic latitude for an assumed value  $EM = 1 \text{ cm}^{-6} \text{ pc}$  towards pulsars at distances  $D = 250 \text{ pc}$  and  $1 \text{ kpc}$ . Upper dashed line: correction for absorption,  $A = e^{0.086/\sin|b|}$ . The standard deviation in  $A$  decreases from 0.16 at  $|b| = 5^\circ$  to 0.05 at  $|b| = 10^\circ$ , 0.02 at  $|b| = 20^\circ$  and  $< 0.01$  at  $|b| > 40^\circ$ . Dot-dashed lines: correction for contributions to EM from beyond the pulsar distance,  $B = 1 - e^{-|z_p|/h}$  with  $h = 280 \text{ pc}$ . For  $h = 500 \text{ pc}$   $B$  is 0.1 to 0.2 lower than the curves shown. The standard deviation in  $B$  is  $< 0.08$  for  $250 < h < 500 \text{ pc}$ . Full lines: corrected emission measure  $EM_p = EM \cdot A \cdot B$ . The errors in  $EM_p$  are typically  $\sim 15\%$ ; they are dominated by the standard deviations in the observed EM. See Sect. 2.3 for further explanations.

$0.13 \text{ cm}^{-6} \text{ pc}^5$ , thus the mean absorption towards the poles is a factor 1.5.

Comparison of Figs. 8a and 8b reveals the much larger spread in  $EM_p$  than in DM. Part of this extra spread arises because fluctuations in electron density influence DM linearly but  $EM_p$  quadratically. The clumpy structure of the dust (Diapas & Savage 1994) leads to variations in absorption and increases the spread in the observed emission measures. Inadequate corrections for absorption and for contributions from beyond the pulsars also enhance the spread in  $EM_p$  compared to that in DM.

### 3.2. Scale heights of $\langle n_e \rangle$ , $\langle n_e^2 \rangle$ , $\bar{n}_c$ and $\bar{f}_v$

The variations of  $\bar{n}_c$  and  $\bar{f}_v$  with height above the Galactic plane are important functions for the understanding of physical processes in the warm ionized disk. Therefore we investigate the dependencies of  $\langle n_e \rangle$ ,  $\langle n_e^2 \rangle$ ,  $\bar{n}_c$  and  $\bar{f}_v$  on  $|z|$  in this section. Although these variables represent averages along the line of sight<sup>6</sup>, we approximate their  $|z|$ -distributions

<sup>5</sup> This value, corresponding to  $0.97 \pm 0.06R$ , is consistent with the mean  $H\alpha$  intensity of the survey of Haffner et al. (2003, their Fig. 13) at  $|b| = 25^\circ$ , the mean latitude of the 130 pulsars in our sample.

<sup>6</sup> Averages along the line of sight are equal to averages along  $|z|$ . For example,  $\langle n_e \rangle = DM/D = DM \sin|b|/|z|$ .

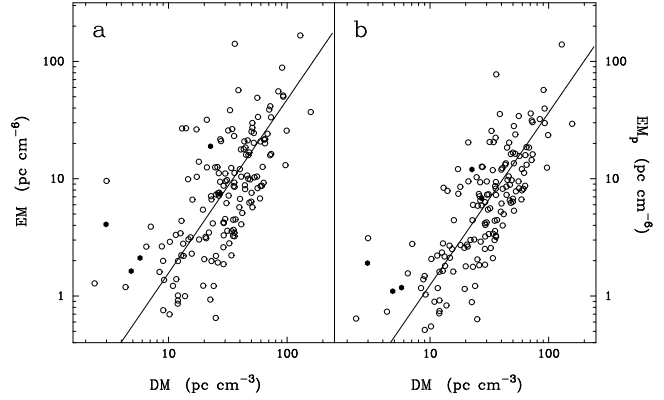


**Fig. 7.** Comparison of emission measure and dispersion measure for the sample of 157 pulsars. **(a)** Observed emission measures, EM. **(b)** Emission measures corrected for absorption and contributions from beyond the pulsar distance,  $EM_p$ . The full lines indicate the bisector fits given in Table 2. Filled circles are pulsars with parallactic distances.

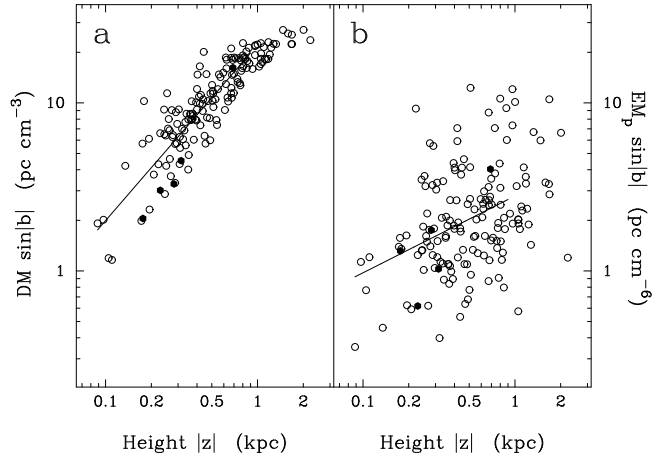


**Fig. 8.** **(a)** Dependence of the dispersion measure perpendicular to the Galactic plane,  $DM \sin|b|$ , on distance above the plane,  $|z|$ . **(b)** Same for the corrected emission measure perpendicular to the plane,  $EM_p \sin|b|$ . Full lines indicate the power-law fits given in Table 2. Filled circles are pulsars with parallactic distances.

by exponentials and estimate the scale heights  $H$ . The relationship between  $H$  and the scale height  $h$  of the local electron density  $n_e^2(z)$  is given by Eq. (9) in Sect. 3.5. Because  $DM \sin|b|(z)$  flattens near  $|z| \simeq 1 \text{ kpc}$  (see Fig. 8a), we determined the scale heights for pulsars at  $|z_p| < 0.9 \text{ kpc}$ . There are 130 pulsars in this sample.

Figure 9 shows the distributions of the various densities and  $\bar{f}_v$  in the  $\ln Y - |z|$  plane. The exponential fits are listed in Table 2.

As the model of Cordes & Lazio (2002) assumes that  $\langle n_e \rangle$  is constant,  $\langle n_e \rangle$  is independent of  $|z|$  (Fig. 9a). The spread in  $\langle n_e \rangle$  is within a factor of 2 to 3 around the mean; the mean value at the midplane  $\langle n_e \rangle_0$  of  $0.0205 \pm 0.0014 \text{ cm}^{-3}$  is in good agreement with earlier determinations for the solar neighbourhood (Reynolds 1991b; Weisberg et al. 1980). The spread decreases steadily with increasing  $|z|$ . This is a

**Table 2.** Statistical relationships for  $h = 0.28$  kpc

X	Y	Function	Kind of fit			corr.coeff. $r$	Student $t$	$ z $ [kpc]	N
				$a$	$b$				
DM	EM	$Y = aX^b$	bis. <sup>1)</sup>	$0.052 \pm 0.020$	$1.48 \pm 0.10$	$0.65 \pm 0.06$	10.7	all	157
DM	$EM_p$	"	"	$0.042 \pm 0.014$	$1.47 \pm 0.09$	$0.76 \pm 0.05$	14.5	"	"
DM cos $ b $	$EM_p \cos  b $	"	"	$0.055 \pm 0.015$	$1.41 \pm 0.07$	$0.85 \pm 0.04$	20.2	"	"
DM sin $ b $	$EM_p \sin  b $	"	"	$0.168 \pm 0.027$	$1.08 \pm 0.06$	$0.44 \pm 0.07$	6.1	"	"
$ z $	DM sin $ b $	"	pow. <sup>2)</sup>	$22.1 \pm 1.3$	$1.04 \pm 0.05$	$0.89 \pm 0.04$	22.3	< 0.9	130
$ z $	$EM_p \sin  b $	"	"	$2.78 \pm 0.28$	$0.46 \pm 0.11$	$0.68 \pm 0.06$	10.6	"	"
$ z $	$\langle n_e \rangle$	$Y = ae^{ z /b}$	exp.+ <sup>3)</sup>	$0.0205 \pm 0.0014$	$14 \dots 8$ <sup>4)</sup>	$0.66 \pm 0.07$	9.8	< 0.9	130
$ z $	$\langle n_e^2 \rangle$	"	" -	$0.0084 \pm 0.0012$	$0.75^{+0.20}_{-0.13}$	$0.71 \pm 0.06$	11.4	"	"
$ z $	$\bar{n}_c$	"	" -	$0.407 \pm 0.059$	$0.71^{+0.18}_{-0.12}$	$0.72 \pm 0.06$	11.8	"	"
$ z $	$\bar{f}_v$	"	" +	$0.0504^{+0.0095}_{-0.0080}$	$0.67^{+0.20}_{-0.13}$	$0.72 \pm 0.06$	"	"	"
$\bar{n}_c$	$\bar{f}_v$	$Y = aX^b$	pow.	$0.0178 \pm 0.0015$	$-1.11 \pm 0.04$	$0.95 \pm 0.03$	33.4	< 0.9	130
				$0.0184 \pm 0.0011$	$-1.07 \pm 0.03$	$0.94 \pm 0.03$	35.1	all	157
$\bar{n}_c$	$L_e$	"	"	$35 \pm 6$	$-0.82 \pm 0.10$	$0.72 \pm 0.06$	11.8	< 0.9	130
				$35 \pm 5$	$-0.86 \pm 0.06$	$0.74 \pm 0.05$	13.6	all	157

1) Bisector in  $\log Y - \log X$  plane. 2) Regression line of  $\log Y$  on  $\log X$ . 3) Regression line of  $\ln Y$  on  $|z|$  with slope  $1/b$ , where  $b$  is the scale height  $H$  in kpc; +/- means increases/decreases with  $|z|$ . All fits are ordinary least-squares fits with errors of one standard deviation. Fits with  $t > 3.1$  are significant at the  $3\sigma$ -level. 4) Error is undefined. Units: DM in  $\text{cm}^{-3}$  pc, EM and  $EM_p$  in  $\text{cm}^{-6}$  pc,  $\langle n_e \rangle$  and  $\bar{n}_c$  in  $\text{cm}^{-3}$ ,  $\langle n_e^2 \rangle$  in  $\text{cm}^{-6}$ ,  $|z|$  in kpc,  $L_e$  in pc.

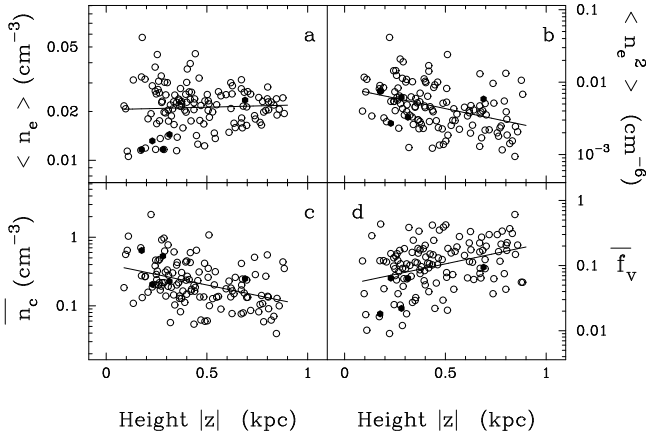


**Fig. 9.** Electron densities averaged along the line of sight and average volume filling factor as function of height above the Galactic plane,  $|z|$ . **(a)** average density  $\langle n_e \rangle = DM \sin |b| / |z|$ . **(b)** average of the square of the density  $\langle n_e^2 \rangle = EM_p \sin |b| / |z|$ . **(c)** mean density in clouds  $\bar{n}_c = EM_p / DM$ . **(d)** average volume filling factor  $\bar{f}_v = DM^2 / (EM_p D)$ . Full lines indicate the exponential fits for  $|z| < 0.9$  kpc given in Table 2. Filled circles are pulsars with parallactic distances.

real  $|z|$ -effect and not just caused by a longer line of sight, because in a plot of  $\langle n_e \rangle - D \cos |b|$  (not shown) the spread in  $\langle n_e \rangle$  remains the same up to a distance of 3 kpc, beyond which only 13 pulsars are located.

Figure 9b shows a decrease of  $\langle n_e^2 \rangle$  with  $|z|$  corresponding to a scale height  $H$  of about 750 pc. The bottom panels of Fig. 9 show the variations of  $\bar{n}_c$  (left) and  $\bar{f}_v$  (right) with  $|z|$ . The exponential fits show that  $\bar{n}_c(|z|)$  decreases with

$H \simeq 710$  pc, whereas  $\bar{f}_v(|z|)$  increases with  $H \simeq 670$  pc. Their midplane values are  $\bar{n}_{c,0} = 0.41 \pm 0.06 \text{ cm}^{-3}$  and  $\bar{f}_{v,0} = 0.050 \pm 0.009$ , respectively (see Table 2). Note that the near equality of the scale heights of  $\langle n_e^2 \rangle$  and  $\bar{n}_c$ , and of  $\bar{f}_v$  with opposite sign, follows from the relations  $\bar{n}_c = \langle n_e^2 \rangle / \langle n_e \rangle$ ,  $\bar{f}_v = \langle n_e \rangle^2 / \langle n_e^2 \rangle$  and the constant value of  $\langle n_e \rangle$  with  $|z|$  (see Eqs. (1) to (4)). The increase of  $\bar{f}_v$  with  $|z|$  could cause the decreasing spread in  $\langle n_e \rangle$  with  $|z|$  as long lines of sight through low-density regions at high  $|z|$  will give less variation in  $\langle n_e \rangle$  than short lines of sight through high-density regions at low  $|z|$ .

We conclude that up to  $|z| = 0.9$  kpc  $\langle n_e \rangle$  the scale heights  $H$  of  $\langle n_e^2 \rangle$ ,  $\bar{n}_c$  and  $\bar{f}_v$  are about 0.7 kpc for this sample of pulsars at  $60^\circ < \ell < 360^\circ$  and  $|b| > 5^\circ$ .

### 3.3. Volume filling factors and $\bar{n}_c$

In Fig. 10 we present the dependence of the volume filling factor  $\bar{f}_v$  on the mean electron density in clouds  $\bar{n}_c$  for all pulsars in the sample ( $N = 157$ ). The correlation is very good: the power-law fit yields  $\bar{f}_v(\bar{n}_c) = (0.0184 \pm 0.0011) \bar{n}_c^{-1.07 \pm 0.03}$  with a correlation coefficient  $r = 0.94 \pm 0.03$  and  $t = 35$  (see Table 2). It nearly covers two orders of magnitude in  $\bar{n}_c$  ( $0.02 - 2 \text{ cm}^{-3}$ ) and  $\bar{f}_v$  ( $0.9 - 0.009$ ). For pulsars at  $|z| < 0.9$  kpc the resulting fit is nearly the same. While an inverse correlation between  $\bar{f}_v$  and  $\bar{n}_c$  is expected from the near constancy of  $\langle n_e \rangle = \bar{f}_v \bar{n}_c$ , the combination of DM and EM yields the values of  $\bar{n}_c$  and  $\bar{f}_v$  for which it holds.

The small spread of about a factor 2 in  $\bar{f}_v$  for a certain  $\bar{n}_c$  is remarkable. This is due to two fortunate facts: 1. since  $\bar{n}_c = EM_p / DM$  and  $\bar{f}_v = DM^2 / EM_p D$ ,  $D$  and er-



rors in  $D$  cancel in both quantities (see Eqs. (1) to (4)), 2. any variation in  $EM_p$ , which causes the largest spread in the various correlations, influences  $\bar{f}_v$  and  $\bar{n}_c$  by the same factor but in opposite directions. Therefore points just slide up or down along the distribution of points with slope  $-1$ . For the same reason the corrections to  $EM$  have little effect on the  $\bar{f}_v(\bar{n}_c)$  relation. Without corrections we find  $\bar{f}_v(\bar{n}_c) = (0.0193 \pm 0.0009)\bar{n}_c^{-1.04 \pm 0.03}$  for  $N = 157$ , which holds for somewhat higher densities ( $0.04 < \bar{n}_c < 4 \text{ cm}^{-3}$ ) than the corrected relation.

The inverse dependence of  $\bar{f}_v$  on  $\bar{n}_c$  obtained here is somewhat steeper than the dependence derived by Pynzar (1993) and Berkuijzen (1998). Their result,  $\bar{f}_v \propto \bar{n}_c^{-0.7}$ , was based on a large variety of data, including classical H II regions, and the pulsar distances were less well known. Without the classical H II regions Pynzar's data indicate a slope closer to  $-1$ . We believe that our coherent data set of 157 pulsars at  $|b| > 5^\circ$  more reliably represents the inverse relationship between  $\bar{f}_v$  and  $\bar{n}_c$  for the diffuse ionized gas. For mean cloud densities in the range  $0.03 < \bar{n}_c < 2 \text{ cm}^{-3}$  we find volume filling factors of  $0.8 > f_v > 0.01$  (see Fig. 10).

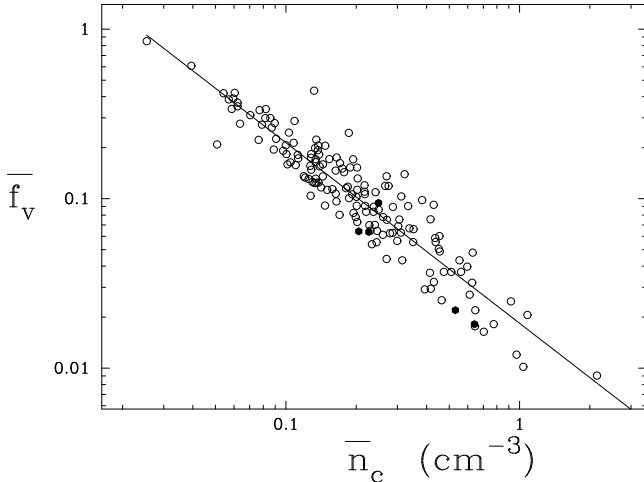


**Fig. 10.** Dependence of the average volume filling factor  $\bar{f}_v$  on the mean density in clouds  $\bar{n}_c$  for the final sample of 157 pulsars. The full line represents the power-law fit  $\bar{f}_v(\bar{n}_c) = (0.0184 \pm 0.0011)\bar{n}_c^{-1.07 \pm 0.03}$ . The correlation coefficient  $r = 0.94 \pm 0.03$  and the Student-t = 35 (see Table 2). Filled circles are pulsars with parallactic distances.

### 3.4. Extent of ionized regions

As the volume filling factor  $\bar{f}_v$  of the DIG increases with decreasing mean density  $\bar{n}_c$ , also an increase of the extent of the ionized regions is expected. This relationship is shown in Fig. 11 where we plotted  $L_e$  as a function of  $\bar{n}_c$  for the total sample of 157 pulsars. A power-law fit yields  $L_e(\bar{n}_c) = (35 \pm 5)\bar{n}_c^{-0.86 \pm 0.06}$  pc with high significance. The extent of the ionized gas along the line of sight towards the pulsars ranges from about 35 pc for  $\bar{n}_c \simeq 1 \text{ cm}^{-3}$  to about 500 pc for  $\bar{n}_c \simeq 0.05 \text{ cm}^{-3}$ . Like in the case of  $\bar{f}_v(\bar{n}_c)$ , the slope of this relationship is insensitive to errors in  $EM_p$ . The spread

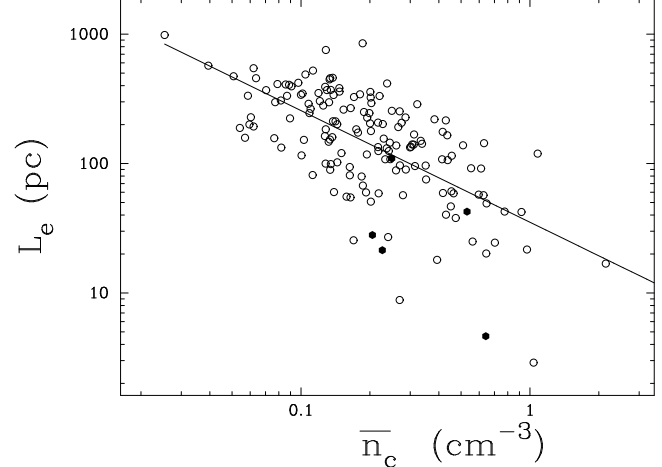


**Fig. 11.** Dependence of the total path length along the line of sight through the ionized regions,  $L_e$ , on the mean density in these regions  $\bar{n}_c$ . The full line represents the power-law fit for the sample of 157 pulsars (see Table 2). Filled circles are pulsars with parallactic distances.

in the distribution of  $L_e(\bar{n}_c)$  is larger than in that of  $f_v(\bar{n}_c)$ , because  $L_e$  still contains the distance  $D$ .

Perhaps more interesting than the extent of the ionized regions towards the pulsars, which depends on their latitude, is their extent in the  $|z|$ -direction. This is best obtained from the relation  $L_e \sin |b|(z) = \bar{f}_v(z)|z|$ .  $L_e \sin |b|$  grows from about 6 pc for  $|z| = 100$  pc to 53 pc for  $|z| = 500$  pc and about 200 pc near  $|z| = 1$  kpc. The corresponding mean densities in the clouds, calculated from  $\bar{n}_c(z)$  given in Table 2, are  $0.35 \text{ cm}^{-3}$ ,  $0.20 \text{ cm}^{-3}$  and  $0.12 \text{ cm}^{-3}$ , respectively.

### 3.5. Dependence of various relationships on $h$

The results presented in Table 2 were obtained using  $h = 0.28$  kpc to correct the observed emission measures for contributions from beyond the pulsar distance (see Eq. 6). However, in Sect. 4.1 we find that  $h$  could be as high as 0.5 kpc. To see how  $h > 0.28$  kpc influences the values in Table 2, we repeated the fitting procedures for  $h = 0.36$  kpc and  $h = 0.5$  kpc.

The correlations  $Y(X)$  corresponding to  $EM_p(\text{DM})$ ,  $EM_p \cos |b|(\text{DM} \cos |b|)$  and  $\bar{f}_v(\bar{n}_c)$  remained the same to within 1 s.d. from the values in Table 2, while those of  $EM_p \sin |b|(\text{DM} \sin |b|)$  and  $EM_p \sin |b|(|z|)$  stayed within 2 s.d. from the values in Table 2. Only the scale heights  $H$  and the midplane values  $Y_0(h)$  of  $\langle n_e^2 \rangle$ ,  $\bar{n}_c$  and  $\bar{f}_v$  changed by  $\gtrsim 2$  s.d. if  $h = 0.5$  kpc is used. For  $0.25 \leq h \leq 0.5$  kpc these values can be found from

$$H(h) = 1.8h + 0.24 \text{ kpc} \quad \text{for } \langle n_e^2 \rangle. \quad (7)$$

The scale heights of  $\bar{n}_c$  and  $\bar{f}_v$  are  $0.95H(h)$  and  $0.89H(h)$ , respectively.

$$\begin{aligned} Y_0(h) &= 1.04Y_0(0.28) * 0.28/h \quad \text{for } \langle n_e^2 \rangle \text{ and } \bar{n}_c, \\ Y_0(h) &= 1.04Y_0(0.28) * h/0.28 \quad \text{for } \bar{f}_v, \end{aligned} \quad (8)$$

where  $Y_0(0.28) = a$  in Table 2.

The general relationship between  $H$  and  $h$  is given by

$$\begin{aligned} \langle n_e^2 \rangle(z) &= \frac{\text{EM}_p \sin |b|(z)}{|z|} = \frac{1}{|z|} \int_0^{|z|} n_e^2(0) e^{-|z|/h} dz \\ &\simeq \langle n_e^2 \rangle_0 e^{-|z|/H}. \end{aligned} \quad (9)$$

As  $\langle n_e^2 \rangle(z)$  is not a purely exponential function, the last expression is only an approximation. Similar relations hold for  $\bar{n}_c$  and  $\bar{f}_v$ . We checked how well this approximation describes the observations by simulating a data set of  $\langle n_e^2 \rangle(z)$  calculated from the integral between  $|z| = 0$  and 0.9 kpc divided by  $|z|$  for  $h = 0.28$  kpc,  $n_e^2(0) = 1 \text{ cm}^{-6}$ , and fitting an exponential to this (noiseless) distribution, exactly as we did in Sect. 3.2. We found  $H = 0.75 \pm 0.02$  kpc and  $\langle n_e^2 \rangle_0 = 0.94 \pm 0.01 \text{ cm}^{-6}$ . The errors and the decrease of 6% in  $\langle n_e^2 \rangle_0$  are caused by the curvature of  $\ln \langle n_e^2 \rangle(z)$  versus  $|z|$ . Thus the simulation yields the same scale height  $H$  as derived from the (noisy) observations (see Table 2) and indicates that the midplane value in Table 2 may be 6% low, which is within the observational errors.

## 4. Discussion

In this section we focus on the vertical structure of the electron layer. We derive the scale height  $h$  of the local electron density in Sect. 4.1, compare this with other scale heights in Sect. 4.2 and discuss the relationship between  $\bar{f}_v$  and  $\bar{n}_c$  in Sect. 4.3.

### 4.1. Vertical structure of the DIG

The variation of  $\langle n_e \rangle$  with  $|z|$  for all pulsars in our sample ( $N=157$ ) is shown in Fig. 12. Below  $|z| \simeq 0.9$  kpc  $\langle n_e \rangle$  is nearly constant (see also Fig. 9a) but beyond this height  $\langle n_e \rangle$  starts decreasing. This variation reflects the linear increase of  $\text{DM} \sin |b|$  up to  $|z| \simeq 0.9$  kpc and its levelling off at higher  $|z|$  observed for various samples of pulsars at known distances (see also Fig. 8a). Such a behaviour of  $\text{DM} \sin |b|(z)$  is expected if the local electron density  $n_e(z)$  decreases exponentially with a scale height of about 1 kpc (Reynolds 1991b; Bhattacharya & Verbunt 1991; Nordgren et al. 1992; Gómez et al. 2001; Cordes & Lazio 2003) which was also adopted by Cordes & Lazio (2002) for their model. However, in an analysis of the dependence of  $\text{DM} \sin |b|$  on  $|z|$  of about 70 pulsars with independent distance estimates, Cordes & Lazio (2003) noted that this dependence may be due to a constant local electron density up to  $|z| \simeq 1$  kpc and that the electron layer may be bounded near this height. Here we give an alternative explanation of the dependence of  $\text{DM} \sin |b|$  on  $|z|$ .

The key observation is the constancy of  $\langle n_e \rangle$  for  $|z| \lesssim 0.9$  kpc. This implies that the local electron density  $n_e(z)$  is also constant and that the local filling factor  $f(z)$  and local density in clouds  $n_c(z)$  are inversely correlated. We expect  $n_c(z)$  to decrease with increasing  $|z|$ . This is indicated by the decrease of emission measure observed for the Perseus arm (Haffner et al. 1999) and external, edge-on galaxies. Hence,

$f(z)$  increases with  $|z|$ . Beyond  $|z| \simeq 0.9$  kpc  $\text{DM} \sin |b|(z)$  flattens and  $\langle n_e \rangle(z)$  starts decreasing (see Fig. 12). We suggest that this occurs because near  $|z| = 0.9$  kpc  $f(z)$  reaches a maximum whereas  $n_c(z)$  continues to decrease beyond this height.  $\text{DM} \sin |b|(z)$  may then be described in the following way:

$$\begin{aligned} \text{DM} \sin |b|(z) &= \int_0^{|z|} n_e(z) dz = \int_0^{|z|} f(z) n_c(z) dz \\ &= \int_0^{|z|} f_0 e^{|z|/h_f} n_{c,0} e^{-|z|/h_n} dz, \end{aligned} \quad (10)$$

where we assumed that  $f(z)$  and  $n_c(z)$  are exponentials with midplane values  $f_0$  and  $n_{c,0}$ , and scale heights  $h_f$  and  $h_n$ , respectively.

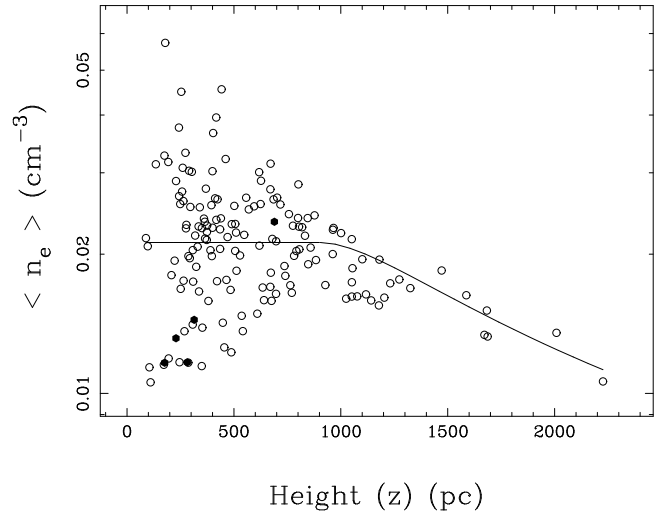


**Fig. 12.** Dependence of the average electron density along the line of sight  $\langle n_e \rangle = \text{DM} \sin |b|/|z|$  on height above the Galactic plane  $|z|$  for the sample of 157 pulsars. The full horizontal line for  $|z| < 0.9$  kpc is at  $\langle n_e \rangle = 0.0213 \text{ cm}^{-3}$ . The continuation to larger  $|z|$  shows the values expected (Eq. (11) divided by  $|z|$ ) for a true scale height  $h = 280$  pc and maximum local filling factor  $f(z_1) = 1$  at  $|z_1| = 0.9$  kpc. See Sect. 4.1 for explanations.

We know that for  $|z| < |z_1| \simeq 0.9$  kpc  $\text{DM} \sin |b|(z) = \langle n_e \rangle |z|$ . Hence  $h_f = h_n = h$ ,  $f_0 n_{c,0} = n_e(0) = \langle n_e \rangle$  and  $f(z) < f(z_1)$  where  $f(z_1)$  is the maximum value. For  $|z| \geq |z_1|$  we have

$$\text{DM} \sin |b|(z) = \langle n_e \rangle |z_1| + f(z_1) \int_{|z_1|}^{|z|} n_{c,0} e^{-|z|/h} dz. \quad (11)$$

Thus for very large  $|z|$   $\text{DM} \sin |b|(z)$  reaches a maximum

$$\text{DM} \sin |b|_{\text{max}} = \langle n_e \rangle |z_1| + f(z_1) n_{c,0} h e^{-|z_1|/h}, \quad (12)$$

where  $|z_1|$  is the height at which the turn-over in  $\text{DM} \sin |b|(z)$  starts and  $f(z_1) = f_0 e^{|z_1|/h}$ .

Similarly, we may describe the emission measure perpendicular to the Galactic plane as

$$\text{EM}_p \sin |b|(z) = \int_0^{|z_p|} n_e^2(z) dz = \int_0^{|z_p|} f(z) n_c^2(z) dz.$$

Since  $f(z)n_c(z) = f_0n_{c,0}$  for  $|z| < |z_1|$  and  $f(z) = f(z_1)$  for  $|z| \geq |z_1|$ , we have

$$\begin{aligned} \text{EM}_p \sin |b|(z) &= f_0 n_{c,0} \int_0^{|z| < z_1|} n_{c,0} e^{-|z|/h} dz \\ &+ f(z_1) \int_{|z_1|}^{|z| > z_1|} n_{c,0}^2 e^{-2|z|/h} dz. \end{aligned}$$

Thus the maximum emission measure through the electron layer is

$$\begin{aligned} \text{EM}_p \sin |b|_{\max} &= \langle n_e \rangle n_{c,0} h \left( 1 - e^{-|z_1|/h} \right) \\ &+ f(z_1) \frac{n_{c,0}^2 h}{2} e^{-2|z_1|/h}. \end{aligned} \quad (13)$$

This is equal to the absorption-corrected emission measure  $\text{EM}_c \sin |b|$  discussed in Sect. 2.3. For  $|z| > |z_1|$  we expect little increase of the emission measure because the second term in Eq. (13) is much smaller than the second term in Eq. (12) and even the dispersion measures increase by  $\lesssim 25\%$  beyond  $|z| = 0.9$  kpc (see Fig. 8a). Therefore we assume that at  $|z| = |z_1|$  the maximum value is nearly reached and reduce Eq. (13) to

$$\text{EM}_p \sin |b|_{\max} = \langle n_e \rangle n_{c,0} h. \quad (14)$$

We can now evaluate the scale height  $h$  by combining Eqs. (12) and (14) with known data. For  $\langle n_e \rangle$  we take the mean value of the slightly sloping function  $\langle n_e \rangle(z)$ ,  $\langle n_e \rangle = f_0 n_{c,0} = 0.0213 \pm 0.0002 \text{ cm}^{-3}$ . The average value of the absorption-corrected emission measures  $\overline{\text{EM}_c \sin |b|} = 3.2 \pm 0.2 \text{ cm}^{-6} \text{ pc}$  (see Sect. 2.3), which gives  $n_{c,0} h = 150 \pm 10 \text{ cm}^{-3} \text{ pc}$ . From Fig. 8a we obtain  $\text{DM} \sin |b|_{\max} = 25 \pm 2 \text{ cm}^{-3} \text{ pc}$  and  $z_1 \simeq 0.9$  kpc. We first take  $f(z_1) = f_0 e^{|z_1|/h} = 1$  which gives a lower limit to  $h$ . For an assumed value of  $h$  we then calculate  $n_{c,0}$ ,  $f_0$ ,  $|z_1|$ ,  $\text{DM} \sin |b|(z_1)$  and  $\text{DM} \sin |b|_{\max}$ . We found  $|z_1|$  and  $\text{DM} \sin |b|_{\max}$  to be in the correct range for  $250 < h < 310$  pc. Repeating the procedure for a more realistic value of  $f(z_1) = 0.5$  yielded a somewhat larger scale height:  $320 < h < 400$  pc (see Table 3). The height  $|z_1|$  decreases when  $h$  increases. The lowest value of  $|z_1|$  consistent with the data in Fig. 8a is  $\simeq 750$  pc. Assuming this value gives an upper limit to  $h$  in the range  $330 < h < 520$  pc and a maximum filling factor of  $0.46 > f(z_1) > 0.31$ . We conclude that the scale height of the local electron density in the DIG is in the range  $250 < h \lesssim 500$  pc and that the maximum filling factor  $f(z_1) > 0.3$ . Because the lower limit to  $h$  is best constrained, we used  $h = 280$  pc to correct the emission measures for contributions from beyond the pulsars in Sect. 2.3. How a larger value of  $h$  changes the results in Table 2 is described in Sect. 3.5.

In Fig. 12 the expected variation of  $\langle n_e \rangle(z)$  is shown for  $h = 280$  pc and  $f(z_1) = 1$ . The agreement with the data at  $|z| > 0.9$  kpc is very good. With  $f(z_1) = 0.5$   $\langle n_e \rangle(z)$  is constant up to  $|z_1| = 820$  pc and then decreases more slowly to the same value at  $|z| = 2$  kpc as for  $f(z_1) = 1$ . Also for  $|z_1| = 750$  pc and  $h = 500$  pc the line is nearly identical to those of the two other cases.

For an electron layer with constant  $\langle n_e \rangle$  up to 1 kpc and then a sudden cutoff, as proposed by Cordes & Lazio (2003),

$\langle n_e \rangle(z) = \langle n_e \rangle(|z| = 1 \text{ kpc})/|z|$  for  $|z| > 1$  kpc. This leads to a somewhat faster decrease in  $\langle n_e \rangle$  at high  $|z|$  than is observed. A more gradual end of the layer seems more realistic and might be in better agreement with the data.

Above we have described that  $\langle n_e \rangle(z)$  will be constant as long as the local filling factor and electron density in clouds are inversely correlated. This correlation breaks down when the filling factor has reached a maximum value of  $\gtrsim 35\%$  near  $|z| = 0.8$  kpc, whereas the electron density in clouds continues to decrease to higher  $|z|$ . This picture is in good agreement with the data in Fig. 12 and shows that the electron layer does not need to be cut off. Why the filling factor reaches a maximum at high  $|z|$  is an interesting question. Pressure balances must play an important role and model calculations will be needed to better understand what is going on near  $|z| = 1$  kpc (see also Sect. 4.3.1).

## 4.2. Scale heights and column densities

In the foregoing section we showed that at heights above the plane  $\lesssim 1$  kpc the scale height of the emission measure equals the scale height  $h$  of the local electron density in clouds  $n_c$ . This happens because the local volume filling factor  $f$  increases with the same scale height leading to  $n_e(z) = \langle n_e \rangle \simeq \text{constant}$  (see Eq. 13). However, at larger heights the filling factor remains constant at the maximum value  $f(z_1)$  and the scale height of the emission measure becomes  $h/2$ , the scale height of  $n_c^2$ . Unfortunately the emission measure scale height is difficult to observe and the available estimates usually refer to  $|z| \lesssim 1$  kpc.

A lower limit to  $h$  comes from radio recombination lines observed between  $\ell = 332^\circ$  and  $83^\circ$  near  $b = 0^\circ$  (Roshi & Anantharamaiah 2000). These lines originate from low-density ( $1 - 10 \text{ cm}^{-3}$ ) ionized gas in envelopes of normal H II regions. The scale height of this gas is  $\gtrsim 100$  pc. H $\alpha$  observations of M 31 (Walterbos & Braun 1994) and other nearby galaxies (Beckman et al. 2002) show that the DIG is concentrated around the H II regions in the spiral arms. The latter authors argue that electrons leaking from bounded H II regions can travel very large distances and could be the origin of the DIG at high  $|z|$ .

Reynolds (1986) estimated the scale height from a comparison of H $\alpha$  intensities towards the poles and a mean value in the Galactic plane. After correction for absorption and scattering he obtained a scale height of about 250 pc (corrected to  $R_\odot = 8.5$  kpc), within the range of our value of  $250 < h < 500$  pc, although he used a very different method.

Berkhuijsen et al. (1997) estimated the scale height of the thermal radio continuum emission at 1.4 GHz, which is unaffected by absorption, using the data of Reich & Reich (1988). The latitude extent of the thermal emission at galactocentric distance  $R \simeq 4$  kpc indicates a scale height of about 350 pc (after correction for the size of the telescope beam).

From H $\alpha$  observations in the direction  $125^\circ < \ell < 152^\circ$  Haffner et al. (1999) derived a scale height of the emission measure of  $500 \pm 50$  pc for distances between 700 pc and 1750 pc from the Galactic plane in the Perseus arm. Because

**Table 3.** Possible range of true scale height  $h$ 

$f(z_1)$	$h$ [pc]	$n_{c0}$ [cm <sup>-3</sup> ]	$f_0$	$ z_1 $ [pc]	DM sin $ b (z_1)$ [cm <sup>-3</sup> pc]	DM sin $ b _{\max}$ [cm <sup>-3</sup> pc]
1 <sup>1)</sup>	250	0.600	0.0355	836	17.7	23.0
	<b>280</b>	0.536	0.0397	904	19.2	25.1
	310	0.484	0.0440	970	20.6	27.1
0.5 <sup>1)</sup>	320	0.469	0.0454	767	16.3	23.2
	<b>360</b>	0.417	0.0511	821	17.5	25.2
	400	0.375	0.0568	870	18.5	27.1
0.46	330	0.455	0.0469	750 <sup>1)</sup>	16.0	23.1
0.36	<b>420</b>	0.357	0.0596	"	"	25.0
0.31	520	0.288	0.0738	"	"	27.1

<sup>1)</sup> assumed value. See Sect. 4.1 for explanations

of various line-of-sight effects the observed emission measures are dominated by gas at heights smaller than the geometrical  $z$ -distances and the authors note that the derived scale height will be too large. This scale height of  $\lesssim 500$  pc will represent a mixture of the true scale height  $h$  expected for  $z < z_1 \simeq 1$  kpc and  $h/2$  expected for  $z > z_1$ , hence  $\lesssim 500$  pc  $< h \lesssim 1000$  pc. We note that beyond the Galactic solar radius the scale height of the gas increases. Our value of  $250 < h \lesssim 500$  pc for  $|z| < |z_1|$  near the Sun would increase to  $300 < h \lesssim 600$  pc at the radius of  $\sim 10$  kpc of the Perseus arm at  $\ell \simeq 135^\circ$  (Merrifield 1992). Thus if the scale height derived for the Perseus arm is more representative for  $z < z_1$  than for  $z > z_1$  it is consistent with our value obtained for the solar neighbourhood, otherwise it would be larger than expected from the value near the Sun.

In view of all these data, the value of the true scale height derived by us,  $250 < h \lesssim 500$  pc for  $|z| < |z_1| \simeq 1$  kpc seems quite plausible for diffuse ionized gas with mean densities in clouds of  $0.03 < \bar{n}_c < 2$  cm<sup>-3</sup> (see Figs. 9c and 10).

In Fig. 13 we plotted the variations of  $\langle n_e \rangle$ ,  $\bar{n}_c$  and  $\bar{f}_v$  with distance from the plane  $|z|$  between 0 and 1 kpc calculated from the fitted exponentials in Table 2 which are based on  $h = 280$  pc. For  $h = 500$  pc the curves of  $\bar{n}_c$  and  $\bar{f}_v$  are flatter, because  $\bar{n}_c(0)$  drops from  $0.41$  cm<sup>-3</sup> to  $0.24$  cm<sup>-3</sup> and  $\bar{f}_v(0)$  increases from  $0.050$  to  $0.084$ , while the values at  $|z| = 1$  kpc do not change significantly. We also plotted the average density along the line of sight of the warm, diffuse HI gas,  $\langle n_{\text{HI,w}} \rangle = N(\text{HI,w})/|z|$ , derived from the work of Diplas & Savage (1994). This decreases faster than  $\bar{n}_c$  because the true exponential scale height  $h$  is only  $195 \pm 5$  pc which corresponds to  $H = 560 \pm 20$  pc. Combining this with the data for  $\langle n_e \rangle$  yields average degrees of ionization of the diffuse gas,  $\bar{I}_w = \langle n_e \rangle / (\langle n_e \rangle + \langle n_{\text{HI,w}} \rangle)$ , between  $0.053 \pm 0.004$  at the midplane to  $0.24 \pm 0.02$  at  $|z| = 1$  kpc. It is remarkable that  $\bar{I}_w(z)$  and  $\bar{f}_v(z)$  are so similar.

Although in Fig. 13  $\langle n_{\text{HI,w}} \rangle$  is everywhere larger than  $\langle n_e \rangle$ , the local density of warm HI,  $n_{\text{HI,w}}$ , drops below the (constant) local electron density  $n_e = f_0 n_{c,0} = \langle n_e \rangle$  at  $|z| \simeq 560$  pc (see Table 4). This height is close to the result

of Reynolds (1991b), who found that the total electron density becomes larger than the total HI density at  $|z| \simeq 700$  pc. This implies that above this height the local degree of ionization  $I_w$  is larger than 0.5.

The column densities towards  $|z| = 1$  kpc of  $\langle n_e \rangle$  and  $\langle n_{\text{HI,w}} \rangle$  are  $N(\langle n_e \rangle) = \text{DM sin } |b| = (0.68 \pm 0.04)10^{20}$  cm<sup>-2</sup> and  $N(\text{HI,w}) = (2.19 \pm 0.06)10^{20}$  cm<sup>-2</sup>. They are similar to the lower values given by Reynolds (1991b). This is understandable because our sample of pulsars traces the diffuse gas at  $|b| > 5^\circ$  located in mainly inter-arm regions.

**Table 4.** Local degree of ionization and volume filling factor

$ z $ [pc]	$n_{\text{HI,w}}$ [cm <sup>-3</sup> ]	$n_e/n_{\text{HI,w}}$ <sup>1)</sup>	$I_w$ <sup>1)</sup>	$f$ <sup>1)</sup>	
0	0.366	0.058	0.055	0.04	0.07
200	0.131	0.16	0.14	0.08	0.11
400	0.047	0.45	0.31	0.17	0.16
600	0.017	1.25	0.56	0.34	0.24
750	0.0078	2.7	0.73	0.58	0.32
800	0.0061	3.5 3.2	0.78 0.76	0.69	0.32
900	0.0036	5.9 4.4	0.86 0.81	0.99	0.32
1000	0.0022	6.8 5.9	0.87 0.85	1	0.32

<sup>1)</sup> Left-hand values for  $h = 280$  pc, right-hand values for  $h = 500$  pc  
 $n_{\text{HI,w}}(z) = 0.366 \exp(-|z|/195 \text{ pc})$  (Diplas & Savage 1994);  
 $I_w = n_e / (n_e + n_{\text{HI,w}})$ ;  
 $n_e(|z| < |z_1|) = f_0 n_{c0} = 0.021 \text{ cm}^{-3}$  and  $n_e(|z| \geq |z_1|) = f(z_1) n_c(z)$ , where  $f(z) = f_0 \exp(|z|/h)$  and  
 $n_c(z) = n_{c0} \exp(-|z|/h)$ .  
 $h = 280$  pc:  $|z_1| = 900$  pc,  $f(z_1) = 1$ ,  $f_0 = 0.04$ ,  
 $n_{c0} = 0.54 \text{ cm}^{-3}$   
 $h = 500$  pc:  $|z_1| = 750$  pc,  $f(z_1) = 0.32$ ,  $f_0 = 0.07$ ,  
 $n_{c0} = 0.30 \text{ cm}^{-3}$

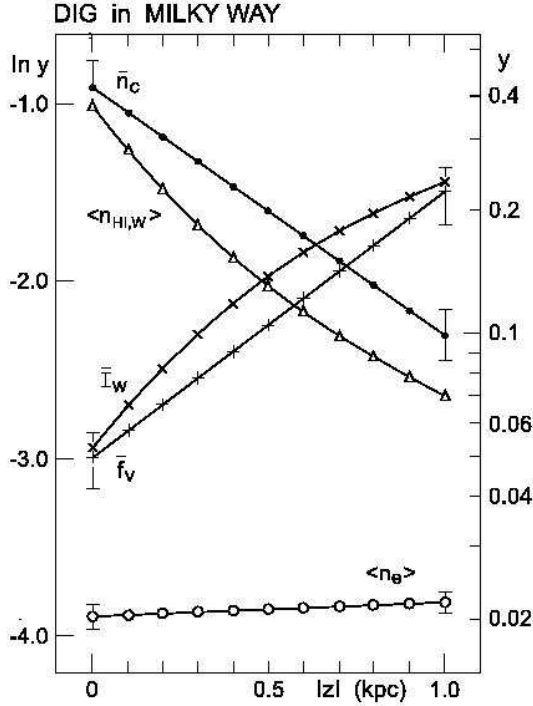


**Fig. 13.** Various quantities averaged along  $|z|$  as a function of height above the Galactic plane. Straight lines are exponential fits given in Table 2. Dots – mean electron density in ionized clouds  $\bar{n}_c = \text{EM}_p/\text{DM}$ . Circles – average electron density  $\langle n_e \rangle = \text{DM} \sin |b|/|z|$ . Triangles – average density of warm diffuse HI,  $\langle n_{\text{HI},w} \rangle = N(\text{HI}, w)/|z|$  taken from Diplas & Savage (1994). Plusses – average volume filling factor  $\bar{f}_v = \text{DM}^2/(\text{EM}_p D)$ . Crosses – average degree of ionization  $\bar{I}_w = \langle n_e \rangle / (\langle n_e \rangle + \langle n_{\text{HI},w} \rangle)$ .  $\text{EM}_p$  was obtained with  $h = 280$  pc. With  $h = 500$  pc the curves of  $\bar{n}_c$  and  $\bar{f}_v$  are flatter than shown. See Sect. 4.2 for explanations.

### 4.3. Volume filling factors

In this section we discuss the dependencies of  $\bar{f}_v$  on  $|z|$  and  $\bar{n}_c$  derived in Sect. 3.2 and possible implications.

#### 4.3.1. Dependence of $\bar{f}_v$ on $|z|$

Figures 9d and 13 show that the volume filling factor averaged along the line of sight increases considerably with height above the Galactic plane. Looking through the electron layer to  $|z| = 1$  kpc,  $\bar{f}_v = 0.22 \pm 0.04$  for  $h = 280$  pc and  $\bar{f}_v = 0.25 \pm 0.04$  for  $h = 500$  pc, values amazingly close to the estimate of  $\bar{f}_v \gtrsim 0.2$  for the full layer made by Reynolds (1991a) based on dispersion measures and emission measures towards 4 pulsars in globular clusters. But this agreement is accidental. Using the method of Kulkarni & Heiles (1988), Reynolds combined the mean values of  $\text{DM} \sin |b|$  and  $\text{EM} \sin |b|$  observed for the 4 pulsars with values of  $\langle n_e \rangle_0$  and  $\langle n_e^2 \rangle_0$  obtained from other sources and did not correct EM for absorption. The combination of data from different sources may introduce errors. Furthermore, as Reynolds noted, the large intrinsic spread in DM and EM and the small number of pulsars make this estimate rather uncertain.

The average ionization degree  $\bar{I}_w$  increases in nearly the same way as  $\bar{f}_v$  (see Fig. 13). If thermal pressure balance exists in the DIG both quantities would increase if the temperature rises with height above the plane. Indications of a temperature increase with  $|z|$  have been reported by Haffner et al. (1999) for the Perseus arm at  $|z| > 700$  pc. Reynolds et al. (1998) found that the ionization ratio  $n_e/n_{\text{HI}}$  is sensitive to temperature. We show this ratio as a function of  $|z|$  in Table 4. Since the filling factor of HI is not known, we calculated the ratio of the local mean densities  $n_e(z) = f(z)n_c(z)$  (see Sect. 4.1) and  $n_{\text{HI},w}(z) = 0.366 \exp(-|z|/195 \text{ pc})$  (Diplas & Savage 1994). Between  $|z| = 0$  and  $|z| = 1$  kpc the ionization ratio increases by more than a factor 100, reaching 1 at  $|z| = 560$  pc. Thus it seems possible that the temperature in the DIG indeed increases with growing distance to the Galactic plane.

In Table 4 we also list the local degree of ionization  $I_w = n_e/(n_e + n_{\text{HI},w})$  and the local filling factors  $f(z)$  for  $h = 280$  pc and  $h = 500$  pc derived in Sect. 4.1. They all increase up to  $|z| = 750$  pc, where  $f(z)$  reaches the maximum value of 0.32 if  $h = 500$  pc. At this height  $I_w = 0.73$ . This high value suggests that the maximum value of  $f(z)$  discussed in Sect. 4.1 occurs when the gas becomes nearly fully ionized. The height above the Galactic plane where this happens is then indicated by the  $|z|$ -distance at which  $\text{DM} \sin |b|(z)$  starts turning over (see Fig. 8a).

#### 4.3.2. Dependence of $\bar{f}_v$ on $\bar{n}_c$

The inverse correlation between  $\bar{f}_v$  and  $\bar{n}_c$ , shown in Fig. 10, is the tightest relationship of the 12 cases listed in Table 2. As explained in Sect. 3.3,  $\bar{f}_v(\bar{n}_c)$  is independent of distance and insensitive to errors in emission measure.

Because both  $\bar{n}_c$  and  $\bar{f}_v$  vary with distance from the Galactic plane (see Figs. 9c and 9d), their correlation could just be a  $|z|$ -effect. However, an inverse relationship is also expected from the constancy of  $\langle n_e \rangle$  with  $D \cos |b|$ , the distance component parallel to the plane:  $\langle n_e \rangle(0) = 0.0206 \pm 0.0009 \text{ cm}^{-3}$  and the slope of the exponential fit in the  $\ln \langle n_e \rangle - D \cos |b|$  plane of  $-0.005 \pm 0.024$ , i.e. effectively zero.

Roshi & Anantharamaiah (2001) made a survey of radio recombination lines of the inner Galaxy at low latitudes. They derived filling factors of  $\lesssim 0.01$  for extended regions of diffuse ionized gas with densities of  $1\text{--}10 \text{ cm}^{-3}$ . Their values are in good agreement with the extension of our relationship in Fig. 10.

We conclude that the inverse relationship between  $\bar{f}_v$  and  $\bar{n}_c$  seems to hold everywhere in the DIG at least for the density range  $0.01 < \bar{n}_c < 10 \text{ cm}^{-3}$ . This general validity shows that it describes a basic property of the DIG, possibly even of the entire ISM (Berkhuijsen 1999). Cordes et al. (1985) estimated a filling factor of  $10^{-4.0 \pm 0.3}$  for clumps of about 1 pc size causing scattering of pulsar signals. The relationships  $\bar{f}_v(\bar{n}_c)$  and  $L_e(\bar{n}_c)$  in Table 2 give  $\bar{f}_v = 1.3 \cdot 10^{-4}$  and  $L_e = 0.8 \text{ pc}$  for  $\bar{n}_c = 100 \text{ cm}^{-3}$ , so these clump properties also seem to follow  $\bar{f}_v \propto \bar{n}_c^{-1}$  derived for the DIG. Furthermore, Gaustad & Van Buren (1993) found a similar relationship between filling factor and mean density for

clouds of diffuse dust within 400 pc from the Sun:  $\bar{f}(\bar{n}_d) = (0.056 \pm 0.020)\bar{n}_d^{-1.25 \pm 0.40}$  for  $1 < \bar{n}_d < 10 \text{ cm}^{-3}$ . For dust densities  $\bar{n}_d = 1 \text{ cm}^{-3}$  and  $10 \text{ cm}^{-3}$  this yields dust filling factors of 0.06 and 0.003, respectively, close to the filling factors of the DIG for the same densities  $\bar{n}_c$ .

Because errors in emission measure hardly influence the  $\bar{f}_v(\bar{n}_c)$ -relation, we also made some fits without any corrections to EM. For the sample  $60^\circ < \ell < 360^\circ$  ( $N = 157$ ) we got the same results as in Table 2 to within the  $1\sigma$ -errors, but the range in  $\bar{n}_c$  extends to  $\bar{n}_c = 4 \text{ cm}^{-3}$ , twice that of the corrected sample, and  $\bar{f}_v$  is correspondingly lower. For our original, full sample of 285 pulsars we find  $\bar{f}_v(\bar{n}_c = 1) = 0.0223 \pm 0.0010$ , exponent =  $-1.02 \pm 0.02$ ,  $r = 0.94 \pm 0.02$  and  $t = 49$ . Even for the small sample of 13 distance calibrators, 5 of which are at  $|b| < 5^\circ$  (see Table 1), we obtain a highly significant inverse correlation in agreement with the larger samples within  $3\sigma$ -errors. Thus also without any corrections to EM a relationship between  $\bar{f}_v$  and  $\bar{n}_c$  with the correct slope can be derived for the DIG, but the individual values of  $\bar{f}_v$  and  $\bar{n}_c$  will be wrong by a factor depending on the pulsar sample.

The inverse relationship between  $\bar{f}_v$  and  $\bar{n}_c$  derived here refers to mainly interarm regions with relatively low average electron density,  $\langle n_e \rangle = 0.021 \text{ cm}^{-3}$ . In spiral arms, where  $\langle n_e \rangle$  seems 2–3 times higher (Cordes & Lazio 2002), correspondingly higher filling factors are expected if the slope of the relation is near  $-1$ .

Which physical process or processes could cause the tight, inverse relationship between  $\bar{f}_v$  and  $\bar{n}_c$ ? Without going into details we mention two possibilities:

- Thermal pressure equilibrium in the DIG. If the temperature increases, the clouds expand and the electron density in clouds decreases. In Sect. 4.3.1 we gave some evidence for an increase of the temperature with  $|z|$ .
- Turbulence in the ISM causing fractal structure. Much of the ISM appears to have fractal structure which leads to  $\bar{f}_v \propto \bar{n}_c^{-1}$  (Fleck 1996; Elmegreen 1998, 1999).

Determinations of the  $\bar{f}_v(\bar{n}_c)$ -relation for other phases of the ISM will be needed to see how widely it is valid. The physical processes causing the inverse relationship  $\bar{f}_v \propto \bar{n}_c^{-1}$  could be studied in simulations modelling the ISM.

## 5. Summary and conclusions

We have used dispersion measures of pulsars (Hobbs & Manchester 2003), distances from the model of Cordes & Lazio (2002) and emission measures from the WHAM survey (Haffner et al. 2003) for a statistical study of several properties of the diffuse ionized gas (DIG) in the Milky Way. The emission measures were corrected for absorption and contributions from beyond the pulsar as described in Sect. 2.3. To avoid regions with excessive absorption and contributions from bright H II regions, we selected pulsars at Galactic latitude  $|b| > 5^\circ$ . The final sample analyzed contains 157 pulsars in the longitude range  $60^\circ < \ell < 360^\circ$ . Their distribution projected on the Galactic plane is shown in Fig. 2. The statistical results are given in Table 2.

Our main conclusions are summarized below.

1. Dispersion measure DM and corrected emission measure  $\text{EM}_p$  are well correlated (Fig. 7b), indicating that they probe the same ionized regions. This allows us to derive and compare the average densities along the line of sight  $\langle n_e \rangle$  and  $\langle n_e^2 \rangle$ , the mean electron density in clouds along the line of sight  $\bar{n}_c$ , the volume filling factor of these clouds  $\bar{f}_v$  and the total path length through the ionized regions  $L_e$  (see Eqs. (1)–(4)).
2. The total extent of the ionized regions perpendicular to the Galactic plane increases from about 6 pc towards  $|z| = 100$  pc to about 220 pc towards  $|z| = 1$  kpc, while the mean cloud density  $\bar{n}_c$  decreases from about  $0.35 \text{ cm}^{-3}$  to about  $0.10 \text{ cm}^{-3}$  (Sect. 3.4).
3. Below  $|z| \simeq 0.9$  kpc  $\langle n_e \rangle$  is essentially constant with a maximum spread of a factor 2 about the mean value of  $0.021 \pm 0.001 \text{ cm}^{-3}$  (Fig. 12). As  $\langle n_e \rangle = \bar{f}_v \bar{n}_c$ , this means that  $\bar{f}_v$  and  $\bar{n}_c$  are inversely correlated. While  $\bar{n}_c$  decreases with increasing  $|z|$  (Fig. 9b),  $\bar{f}_v$  increases with  $|z|$  (Fig. 9d). We derived the relation  $\bar{f}_v(\bar{n}_c) = (0.0184 \pm 0.0011)\bar{n}_c^{-1.07 \pm 0.03}$ , which is very tight. Figure 10 shows that it holds for the ranges  $0.03 \lesssim \bar{n}_c < 2 \text{ cm}^{-3}$  and  $0.8 \gtrsim \bar{f}_v > 0.01$ . The inverse dependence of  $\bar{f}_v$  on  $\bar{n}_c$  could mean that the DIG is in thermal pressure equilibrium or that it has a turbulent, fractal structure.
4. The linear increase of  $\text{DM} \sin |b|$  with  $|z|$  up to  $|z| \simeq 0.9$  kpc indicates that the local electron density  $n_e(z)$  is constant, so also locally  $n_c(z)$  and  $f(z)$  are inversely correlated. We suggest that the turn-over of  $\text{DM} \sin |b|$  near  $|z| = 0.9$  kpc occurs when  $f(z)$  reaches a maximum value, whereas  $n_c(z)$  continues to decrease towards higher  $|z|$  causing a flattening of  $\text{DM} \sin |b|(z)$ .
5. Using this interpretation and the mean of the absorption-corrected emission measures through the full layer  $\overline{\text{EM}_c \sin |b|}$ , we derived a true scale height of  $n_c(z)$  and  $f(z)$  between 250 pc and  $\simeq 500$  pc for maximum values of  $f(z)$  between 1 and 0.3, respectively, near  $|z| \simeq 1$  kpc. Since  $n_e^2(z) = f(z)n_c^2(z)$  and  $n_e(z) = f(z)n_c(z)$  is constant,  $n_e^2(z)$  has the same scale height as  $n_c(z)$  (Sect. 4.2). Beyond  $|z| \simeq 1$  kpc, where  $f(z) \simeq \text{constant}$ , the scale height of  $n_e^2(z)$  becomes a factor of 2 smaller than that of  $n_c(z)$ .
6. The variation of  $\bar{f}_v(z)$  is similar to that of the average degree of ionization of the warm, atomic gas,  $\bar{I}_w(z)$  (Fig. 13). Towards  $|z| = 1$  kpc  $\bar{f}_v = 0.24 \pm 0.05$  and  $\bar{I}_w = 0.24 \pm 0.02$ . The increase of  $\bar{I}_w$  with  $|z|$  may point to an increase of the temperature in the DIG with increasing distance to the Galactic plane. The local function  $I_w(z)$  reaches values near unity at  $|z| = 1$  kpc (Table 4). If  $f(z)$  reaches a maximum value when the gas is nearly fully ionized, then the  $|z|$ -distance where this occurs is indicated by the turn-over point of  $\text{DM} \sin |b|(z)$ .

As the tight inverse relation between  $\bar{f}_v$  and  $\bar{n}_c$  is independent of  $|z|$  or distance along the plane, it seems a basic property of the DIG. Simulations modelling the DIG may be able to reproduce this relationship.

*Acknowledgements.* We thank Dr. A. Fletcher for useful discussions and careful reading of the manuscript, and an anonymous referee for very extensive comments leading to improvement of the paper.

The Wisconsin H-Alpha Mapper is funded by the National Science Foundation.

## References

- Beckman, J. E., Zurita, A., Rozas, M., Cardwell, A., Relaño, M.: 2002, in: S. & M. Torres-Peimbert (ed.), *Ionized Gaseous Nebulae*, Rev. Mex. Astron. Astrofis. (Conf. Ser.) 12, 213
- Berkhuijsen, E. M.: 1998, in: D. Breitschwerdt, M. J. Freyberg, & J. Trümper (ed.), *The Local Bubble and Beyond*, Lecture Notes in Physics, Springer, 301
- Berkhuijsen, E. M.: 1999, in: M. Ostrowski & R. Schlickeiser (ed.), *Plasma Turbulence and Energetic Particles in Astrophysics*, Krakow, Astron. Obs. Jagiellonian Univ., 61
- Berkhuijsen, E. M., Horellou, C., Krause, M., et al.: 1997, A&A 318, 700
- Bhattacharya, D., Verbunt, F.: 1991, A&A 242, 128
- Brisken, W. F., Benson, J. M., Goss, W. M., Thorsett, S. E.: 2002, ApJ 571, 906
- Cordes, J. M., Lazio, T. W. J.: 2002, astro-ph/0207156
- Cordes, J. M., Lazio, T. W. J.: 2003, astro-ph/0301598
- Cordes, J. M., Weisberg, J. M., Boriakoff, W.: 1985, ApJ 288, 221
- Dame, T. M., Hartmann, D., Thaddeus, P.: 2001, ApJ 547, 792
- Dickey, J. M.: 1993, in: R. M. Humphreys (ed.), *Minnesota Lectures on Structure and Dynamics of the Milky Way*, ASP Conf. Ser. 39, 93
- Dickey, J. M., Lockman, F. J.: 1990, ARA&A 28, 215
- Dickinson, C., Davies, R. D., Davis, R. J.: 2003, MNRAS 341, 369
- Diplas, A., Savage, B. D.: 1994, ApJ 427, 274
- Elmegreen, B. G.: 1998, Proc. Astron. Soc. Aust. 15, 74
- Elmegreen, B. G.: 1999, in: V. Ossenkopf, J. Stutzki, & G. Winnewisser (ed.), *The Physics and Chemistry of the Interstellar Medium*, 3rd Cologne-Zermatt Symposium, Aachen, Shaker-Verlag, 77
- Ferrière, K.: 1998, ApJ 497, 759
- Fleck, R. C.: 1996, ApJ 458, 739
- Gaustad, J. E., Van Buren, D.: 1993, PASP 105, 1127
- Gómez, G. C., Benjamin, R. A., Cox, D. P.: 2001, AJ 122, 908
- Haffner, L. M., Reynolds, R. J., Tufte, S. L.: 1998, ApJ 501, L83
- Haffner, L. M., Reynolds, R. J., Tufte, S. L.: 1999, ApJ 523, 223
- Haffner, L. M., Reynolds, R. J., Madsen, G. J., et al.: 2003, ApJS 149, 405
- Heiles, C., Reach, W. T., Koo, B. C.: 1996, ApJ 466, 191
- Hobbs, G. B., Manchester, R. N.: 2003, <http://www.atnf.csiro.au/research/pulsar/psrcat>
- Isobe, T., Feigelson, E. D., Akritas, M. G., Babu, G. J.: 1990, ApJ 364, 104
- Kulkarni, S. R., Heiles, C.: 1988, in: G. A. Verschuur, & K. I. Kellermann (ed.), *Galactic and Extragalactic Radio Astronomy*, New York, Springer, 95
- Lucke, P. B.: 1978, A&A 64, 367
- Merrifield, R. M.: 1992, AJ 103, 1552
- Miller, M. W. III, Cox, D. P.: 1993, ApJ 417, 579
- Mitra, D., Wielebinski, R., Kramer, M., et al.: 2003, A&A 398, 993
- Nordgren, T. E., Cordes, J. M., Terzian, Y.: 1992, AJ 104, 1465
- Pynzar, A. V.: 1993, Astron. Rep. 37, 245
- Reich, P., Reich, W.: 1988, A&A 196, 211
- Reynolds, R. J.: 1977, ApJ 216, 433
- Reynolds, R. J.: 1986, in: J. N. Bregman, & F. J. Lockman (ed.), *Gaseous Halos of Galaxies*, Greenbank, NRAO, 53
- Reynolds, R. J.: 1989, ApJ 339, L29
- Reynolds, R. J.: 1991a, ApJ 372, L17
- Reynolds, R. J.: 1991b, in: H. Bloemen (ed.), *The Interstellar Disk-Halo Connection in Galaxies*, IAU Symp. 144, Dordrecht, Kluwer, 67
- Reynolds, R. J., Hansen, N. R., Tufte, S. L., Haffner, L. M.: 1998, ApJ 494, L99
- Roshi, D. A., Anantharamaiah, K. R.: 2000, ApJ 535, 231
- Roshi, D. A., Anantharamaiah, K. R.: 2001, ApJ 557, 226
- Schlegel, D. J., Finkbeiner, D. P., Davis, M.: 1998, ApJ 500, 525
- Sherwood, W. A.: 1974, Publ. Roy. Obs. Edinburgh 9, 95
- Taylor, J. H., Cordes, J. M.: 1993, ApJ 411, 674
- Taylor, J. H., Manchester, R. N., Lyne, A. G.: 1993, ApJS 88, 529
- Walterbos, R. A. M., Braun, R.: 1994, ApJ 431, 156
- Weisberg, J. M., Rankin, J., Boriakoff, V.: 1980, A&A 88, 84

**Appendix A: Glossary**

$A$	absorption correction applied to EM
$B$	correction for emission measure from beyond the pulsar
$D$	distance to pulsar
DM	observed dispersion measure
EM	observed emission measure
$EM_c$	EM corrected for absorption, $EM_c = EM \cdot A$
$EM_p$	EM corrected for absorption and contributions from beyond the pulsar, $EM_p = EM \cdot AB$
$f$	local volume filling factor
$f_D$	fraction of line of sight containing electrons
$\bar{f}_v$	average volume filling factor, average fraction of radio beam up to pulsar containing electrons
$H$	exponential scale height of quantities averaged along the line of sight
$h$	true scale height, exponential scale height of local quantities
$I_w$	local degree of ionization of warm H I
$\bar{I}_w$	degree of ionization of warm H I averaged along the line of sight
$L_e$	total path length through ionized regions along $D$
$n_c$	local electron density in a cloud
$\bar{n}_c$	mean electron density within clouds
$n_e$	local electron density, $n_e = fn_c$ and $n_e^2 = fn_c^2$
$\langle n_e \rangle$	average electron density along the line of sight, $\langle n_e \rangle = \bar{f}_v \bar{n}_c$
$\langle n_e^2 \rangle$	average along the line of sight of the square of the local electron density, $\langle n_e^2 \rangle = \bar{f}_v \bar{n}_c^2$
$n_{HI,w}$	local density of warm H I
$\langle n_{HI,w} \rangle$	density of warm H I averaged along the line of sight
$z$	height above the Galactic plane
$z_p$	height of the pulsar
$z_1$	height at which $f$ reaches its maximum value